OsloMet – Metropolitan University

Department of Civil Engineering and Energy Technology
Postadresse : P.O. Box 4 St. Olavs plass, 0130 Oslo
Visiting Address: Pilestredet 35, Oslo

Telephone: 67 23 50 00
www.oslomet.no

Master's thesis

TITLE Earthquake Response Analyses of Bi-linear Pile Supported Superstructures	DATE 27.11.20
	PAGES / ATTACHMENTS 61 / 7
AUTHOR Stian Ausland	SUPERVISOR Emrah Erduran

SUMMARY

The investigation in this thesis is related to the structural response of a system supported by piles designed with properties which include inelastic behaviour. This is conducted by comparing the results from simulated models in SAP2000 with elastic and inelastic properties, which get exposed to an earthquake load. The analysed structure is a shear wall from a performed case study of a typical Norwegian apartment building. The seismic event is implemented to the systems according to NS-EN 1998-1-1, appendix B. This method uses the static pushover curve for the equivalent SDOF system of the analysed structure to calculate the response. A parameter study is conducted to investigate how piles designed with perfect elastoplastic properties influence the entire structure. The investigation concludes that designing for inelastic behaviour of piles exposed to an earthquake seems to improve the behaviour of the structure, given certain conditions.

3 KEYWORDS
Seismic event
Pile Foundations
Perfect elastoplastic behaviour

Acknowledgements

This master thesis concludes my Master of Science in Structural Engineering and Building Technology at Oslo Metropolitan University (OsloMet) in the autumn of 2020.

I would like to thank my supervisor Emrah Erduran, Associate Professor at Oslo Metropolitan University, for valuable discussions and constructive feedback. Your eagerness to always help and willingness to engage in my work have been an essential contribution to the final result.

Oslo, November 27, 2020

Stian Ausland

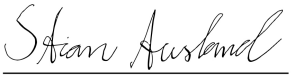

Abstract

The use of piles is a widespread support system for superstructures located on unstable surfaces, which have strict behavioural requirements. The requirements from Eurocode 8 for pile supports is that they have to be designed to remain elastic. The investigation in this thesis is related to the structural response of a system supported by piles designed with insufficient properties, i.e. designed with properties which include inelastic behaviour. This is conducted by comparing the results from simulated models in SAP2000 with elastic and inelastic properties, which get exposed to an earthquake load. The analysed structure is a shear wall from a performed case study of a typical Norwegian apartment building. The seismic event is implemented to the systems according to NS-EN 1998-1-1, appendix B. This method uses the static pushover curve for the equivalent SDOF system of the analysed structure to calculate the response. A parameter study is conducted to investigate how piles designed with perfect elastoplastic properties influence the entire structure. This is done by investigating the results from the SAP2000 models, where the chosen parameters are inserted and changed between each case. The findings in this thesis are based on the results of the parameter study. The findings are done by comparing the results with the response of the superstructure supported by elastic piles. The applied parameters are the total capacity of the support system, λ, and the reduced capacity of the two piles in the middle of the wall, ι. The reduced capacity ι is a percentage reduction of the estimated reaction force for one elastic pile. The parameter study consists of four main sections, where the total capacity of the system, λ, changes between each section. The calculated requirement for the elastic support system is applied as a baseline to give the systems sensible capacities. Further, the main sections are divided into four subsections, based on the degree of ι. Through this parameter study, a general finding is that all the investigated system remains stable. Nevertheless, some of the systems get permanent displaced because of inelastic behaviour, but the total capacity of the supports is not exceeded. If perfect elastoplastic piles are applied with one of the total capacities in the parameter study, this seems to give an improved response regarding the roof displacement. It has also been found that piles described with perfect elastoplastic properties remain elastic if the ι value is set to the lowest percentage reduction investigated. Designing for perfect elastoplastic properties also give a lower total base shear if the system is designed with a total capacity λ 10 $\%$ lower than the estimated requirement for the elastic supported system. The conducted investigation leads to the conclusion that designing for inelastic behaviour of piles exposed to an earthquake seems to improve the structural behaviour, given certain conditions.

Table of Contents

List of Tables

List of Figures

Chapter 1

Introduction

According to Rønnquist et al. (2012), Norway is a country where earthquakes infrequently occur, estimated to occur every 475 years with a magnitude of 6,5 on the Richter scale (EN et al. (2004)). Nevertheless, the costs and consequences related to the occurrence of earthquakes, makes it necessary to design the structure to withstand this cyclic lateral load, depending on the ground conditions.

Piles are frequently used to stabilize structures when located in areas where the steady bedrock is not directly available. In general, piles have to be designed to handle static loading and dynamic earthquake-induced loads, even for constructions in low-seismic regions. To satisfy EN 1998-5:2004, also called Eurocode 8 (EC8), the piles have to be designed based on conservative assumptions, i.e., kept within the elastic range throughout the seismic event (EN et al. (2004)). This requirement makes construction projects more expensive since the lateral capacity has to be strengthened, e.g., by increasing the pile diameter. The requirement of piles' elastic behaviour during an earthquake excludes that inelasticity could positively impact the superstructure and on the pile foundation. If this could be proven wrong, the outcome could be reduced material use and decreased cost for the builder. Therefore, it is of interest, both for contractors and the environment, to inspect the effect of allowing a superstructure and its foundations to behave inelastically.

1.1 Research objective

The dimensioning criteria for piles in EC8, part 5, point 5.4.2 (7) is formulated as follows:
Piles should in principle be designed to remain elastic, but may under certain conditions be allowed to develop a plastic hinge at their heads (EN et al. (2004)).

This study intends to examine the response of a superstructure in Norway exposed to a seismic event and supported by piles with insufficient properties according to the EC8, i.e., designed for inelastic behaviour. The research objective of this thesis is:

Investigate whether designing for inelastic behaviour of piles exposed to an earthquake gives acceptable results regarding the structural behaviour.

This is detected by comparing the behaviour of a structure supported by piles kept within the elastic range with equivalent cases where the piles are allowed to behave inelastically.

1.1.1 Objectives

The following objectives have to be completed in order to answer the research objective:

1. Conduct 2D linear modal analyzes of superstructures and their foundations.
2. Analyse relevant structures through dynamic pushover analyzes.
3. Determine earthquake loads that are based on the modal- and pushover analyzes.
4. Compare the response of the determined earthquake loads for pile foundations with varying degrees of inelastic properties with supports that remains elastic.

The pile foundation is modelled as springs with linear and bi-linear properties, for the elastic and inelastic piles respectively. It is also necessary to calculate spring stiffnesses, which are equal for elastic and bi-linear behaviour.

1.2 Research boundaries

The only analyzed soil type is clay since this is typical for Norwegian construction sites. Consequently, liquefaction of soil is not included. The piles and the superstructure are modelled as 2D elements, and the horizontal forces are assumed to appear only in the inspected 2D plane. Kinematic pile-soil-structure interaction and a bending moment of the piles are not analyzed in this thesis. The only construction part examined in this project is the shear wall and its interaction with the pile foundation. Only the displacement distribution from the mode shape with the largest mass participation ratio is applied in the SAP2000.

1.3 Literature Review

Research on buildings exposed to earthquakes is essential to secure human lives and maintain buildings and infrastructure through seismic events. In this chapter, a literature review has been conducted to understand the method of pile design better and detect the behaviour of piles that behave inelastically. This information will be essential for the research method and analysis of the results.

To design piles for seismic loads, the ultimate lateral capacity of the pile has to be found. Literature regarding this subject is reviewed initially. To find out whether the capacity is sufficient, the pile-soil interaction has to be described in an adequate matter. Therefore, research work concerning the lateral response estimation is rendered in the next subsection. This is followed by a subsection dealing with a description of piles' nonlinear behaviour, which is found relevant since the pile design in this thesis is meant to reach the inelastic zone.

Ultimate lateral capacity of piles

In the research papers written by Bengt B. Broms, the lateral pile capacity in cohesive- ((Broms (1964a)) and cohesiveless soil (Broms (1964b)) were estimated. Both these papers provide descriptions of simple methods to estimate the ultimate lateral pressure with depth, distributed from the soil. The pile caps' characterization supported by the fixed and free head is given, based on whether the pile is short or long. Short piles are controlled regarding the point of failure of the surrounding soil because of the rigidity of the pile. For long piles, the point of interest is the pressure required to reach structural failure.

Kulhawy and Chen (1995) has conducted laboratory field tests to evaluate the methods where lateral capacity is estimated, presented by Broms. It was found that these methods are generally conservative but could achieve accurate results if the calculated values were empirically adjusted.

Soil with linearly increasing strength with depth was, according to Pender (1993), not described in any of the papers by Bengt B. Broms. These are typical properties of soft clay and e.g., covered in Budhu and Davies (1988). In this paper, a parametric study is done to explore how soil yielding for soft clay affects a single pile's load response, which is the topic for the next section of this chapter. The research paper also provides relevant values to use in the calculation of the

ultimate lateral loading.

An alternative approach to calculating the lateral pile capacity with depth is conducted by Reese et al. (1974). This method is more complicated than the method found in the papers by Broms, e.g., since the failure types are assumed to vary at different points downward the pile shaft. Kulhawy and Chen (1995) evaluated that this method estimates the capacity to be lager than found in executed tests.

Lateral response estimation

The work conducted by Gazetas and Makris (1991) expresses a method for computing the dynamic foundation stiffness valid for pile groups and single piles exposed to inertial loading. This is done through a lateral response estimation, where the single pile was modeled as a beam with linear elastic properties embedded in the soil. The soil was represented by Winkler springs. The series of steps also include solving the steady-state harmonic equation of the lateral loaded pile system. Research has shown that SSI has to be included to perform a correct description of the structural behaviour of the building the earthquake event (Jarernprasert et al. (2013), Raychowdhury (2011)). This interaction also gives structures an increased natural period (Sharma et al. (2018), Bi et al. (2011)).

A model which has similarities with the one from Gazetas and Makris (1991) is brought up by El Naggar and Novak (1996). Winkler springs are used along the pile shaft for the implementation of nonlinear soil behaviour. The pile shaft is set to have a circular cross-section, and the shaft is divided into segments with the same length as the distance between each Winkler spring. Each element is given its own structural stiffness matrix, i.e., a standard 4x4 bending matrix. The model also includes the effect of slippage and gapping between the pile shaft and the surrounding soil, called discontinuity conditions. This is a computationally efficient model where only relevant degrees of freedom are included. In order to validate the results, findings from field tests and other analytical solutions are compared with the output from this method. It is found that the calculated lateral dynamic response has adequate similarities with the measured values from the field tests. Another result is that the level of loading affects the single pile stiffness and damping parameters.

Pushover analysis

Performance-based seismic design is a method which, according to Eurocode 8 is originated from inelastic displacement (EN et al. (2004)). Estimation of the nonlinear seismic response

of buildings is an important task in this design approach. This could either be conducted by the nonlinear time-history analysis or through pushover analysis (Chopra and Goel (1999)). The pushover analysis is a method to provide load-displacement and moment-rotation curves of the superstructure and is further described in section **??**. Many research projects related to this analysis has been conducted, i.e., discussing the validity of the results coming from the pushover analysis. It was, e.g., found in Skokan and Hart (2000) that the pushover analysis gives adequate estimations of seismic demands after the structure yields, even though the load distribution applied to this method is based on an unchanged mode shape after the instant of yielding. This scope is restricted to low- and medium-rise structures, according to Gupta and Krawinkler (1998) and Krawinkler and Seneviratna (1998). This is also stated in Mwafy and Elnashai (2001), but here the pushover analysis is restricted to fit symmetric low-rise buildings with a high natural frequency. According to Kunnath and Erduran (2008), the weaknesses of the pushover analysis is that dynamic effects, such as inertia effects, degradation, and damping, are not implemented. Nevertheless, Krawinkler and Seneviratna (1998) has found that the application of pushover analysis can reveal areas where inelastic deformation appears within a critical level.

Nonlinear lateral pile-soil interaction

In Davies and Budhu (1986) the researchers modified the elastic analysis to apply for the local failure of soil with constant stiffness. This is done to calculate the lateral load to which the pile gets exposed when the surrounding soil fails at a given point. The assumption made to take the local failure into account is increased lateral pressure to the pile by adding the length of e_0 to the eccentric lateral load. Before this approach was proposed, Pender (1993) tells that there was no possibility to examine nonlinear behaviour without the application of nonlinear finite element computer programs. Research has also been made on soil with varying soil modulus, e.g., Budhu and Davies (1987) where the soil stiffness increases linearly from the ground surface, but this is not further described in this thesis.

Kunnath et al. (1990) had great progress in his work regarding describing non-linearity for macro-models. The model did, in general, predict the outcome of the structural response of seismic events sufficiently when the response of the system was independent of the foundation. Nevertheless, the result was not valid to the same extent when the foundation influenced the system response. The foundation-structure interaction is properly included in the research work by Ciampoli and Pinto (1995), where the pile and the superstructure were modeled as a vertically rotated cantilever with a lumped mass at the top. The inelastic behaviour is included in

the model by plastic hinges located at prescribed areas. For this model, the drawback is related to the flexibility of the model since the researchers used equivalent damping coefficients to describe the foundation response.

Badoni and Makris (1997) state that to avoid the problems described in the above subsection, the Bouc-Wen model is a sufficient alternative. In the Bouc-Wen model, the superstructure and the foundation are interconnected through nonlinear springs and is found to be an adjustable method to describe macro-models (Bouc (1971)).

1.4 Thesis outline

This thesis contains six main chapters, including the current chapter:
Chapter 2: Theory describes the theory related to the Eigenvalue problem, Eurocode 8, Soil-structure interaction, Design of piles under seismic loading, Winkler foundation Modeling and the p-y curve.

Chapter 3: Methodology presents the applied research methodology and the method applied to determine the earthquake load.

Chapter 4: Case study describes the case study, the setup of the SAP2000 model, applied loads and magnitude of elastic response spectrum. This gives the starting point for the analyses.

Chapter 5: Analysis and Result describes the conducted analyses. These are divided based on the investigated support systems, i.e. pinned, elastic spring, elastic and bi-linear spring and bi-linear spring. The pinned support is involved to see if the models behave realistically.

Chapter 6: Discussion and Conclusion explains the significance of the results from the parameter study and concludes based on the research objective. Suggestions related to future work are also given.

Chapter 2

Theory

The first section of this chapter is related to the eigenvalue problem. This theory is relevant regarding the modal analyses presented in section 3.3. Thereafter, the soil-structure interaction is reviewed, which involves the substructure approach and a description of the dynamic response of single piles. After that, the design process of piles under seismic loading is characterized. This section involves the application of Winkler springs. The Winkler springs make the theory related to the p-y curve relevant.

2.1 Eigenvalue problem

The eigenvalue problem is described in Chopra (2017) as a method to find the size of the natural vibration frequencies and the mode shapes of a multi-degree of freedom (MDOF) structure. The mathematical description of this problem is based on the equation of motion for a structural system with MDOF and free vibration (Chopra (2017)). The equation of motion for this system is expressed as follows:

$$m\ddot{u} + ku = 0 \tag{1}$$

In equation 1 the system undergoes harmonic motions, i.e., the whole structure oscillates with the same natural circular frequency, ω_{n}. The total deflection at the time t, $q_{\mathrm{n}}(t)$, consists of oscillation contributions from every natural frequency. Every natural circular frequency caused by the vibration from the harmonic motion gives a specific mode shape. The displacement from one of the modes shapes, which changes with time t, is given by the following equation:

$$u(t) = q_{\mathrm{n}}(t)\Phi_{\mathrm{n}} \tag{2}$$

where Φ_n is a constant vector which express one of the natural mode shapes (Chopra (2017)). The harmonic motion of a system is described as follows:

$$q_n(t) = A_n cos\omega_n t + B_n sin\omega_n t \tag{3}$$

where A_n and B_n are constants based on the initial conditions of the oscillation. Application of equation 3 for q_n in equation 2 gives

$$u(t) = \Phi_n(A_n cos\omega_n t + B_n sin\omega_n t) \tag{4}$$

This mathematical expression is inserted into equation 1, where the second derivative of equation 5 is applied to describe the acceleration (Chopra (2017)). This leads to the following expression:

$$\big[-{\omega_n}^2 m\Phi_n + k\Phi_n \big] q_n(t) = 0 \tag{5}$$

which can be satisfied either if there is no oscillation in the structure, i.e. $q_n(t) = 0$, or if the natural frequencies and modes fulfill the following condition:

$$\big[k - {\omega_n}^2 m\big]\Phi_n = 0 \tag{6}$$

This algebraic equation is called the eigenvalue problem, and the solutions of this problem are nontrivial if:

$$det\big[k - {\omega_n}^2 m\big] = 0 \tag{7}$$

where the solution, ω_n, is called the eigenvalues and the natural modes Φ_n are corresponding to this natural vibrating frequency (Chopra (2017)).

2.2 Soil-structure interaction

The soil-structure interaction (SSI) is a responsive effect where the superstructure, the pile foundation, and the embedded soil interact during seismic events. This could be modeled through the substructure approach (Jia (2018)).

2.2.1 Substructure approach

The substructure approach is a computationally efficient method to estimate the response of the total response of a structure to a seismic event. This is done through partitioning elements

involved in the soil-structure interaction. It is assumed that the response of the seismic event consists of two different interactions, which are the kinematic and the inertial interaction. Here, the inertial interaction is the main focus for civil engineers (Jia (2018)).

2.2.1.1 Kinematic interaction

The Kinematic interaction is applied to compute the response of the ground. The presence of the foundation in the soil prevents the ground from following its free-field motion, which leads to kinematic interaction. In order to model this, the foundation is assumed to be massless (Jia (2018)).

Eurocode 8 part 5, chapter 5.4.2, demands only calculation of bending moments that occurs as a result of kinematic interaction when the building is located in areas categorized as a zone of moderate or high seismicity and the superstructure is of importance class III (EN et al. (2004)). Since Norway is categorized to have a low-to-moderate seismicity level, the calculation of kinematic interaction will not be calculated in this thesis.

2.2.1.2 Inertial interaction

The examination of the inertial interaction of a single pile involves the application of dynamic loads to the pile head. These loads come both as a result of the ground motion, caused by the seismic event, and the dead load of the superstructure (Pender (1993)). According to Stewart et al. (1999) are the inertial loads providing base shear and overturning moment. As a result of this is the structure subjected to displacements relative to the foundation and the free-field. Frequency functions are applied to describe the pliableness of the pile foundation and the damping effect from the soil-structure interaction (Stewart et al. (1999)).

2.3 Design of Piles Under Seismic Loading

To design end bearing piles to resist earthquake loads, the ultimate lateral capacity of the pile is important because the earthquake is assumed to perform as a horizontal load only. Pender states in his paper that the ultimate lateral capacity of long piles depends on the bending moment capacity of the pile shaft and the support of the pile head. Under conditions where large deformations occur, the outcome is inelastic pile behaviour. This results from yielding of the pile section and can be modeled by inserting plastic hinges at areas where plastic deformation has occurred, to the elastic model. The pile has reached its maximum capacity, and further

loading is therefor making the pile to rotate freely where plastic hinges have been formed (Pender (1993)). According to Broms (1964a) the number of plastic hinges that has to be formed before the pile is categorized as a mechanism is determined by the pile head support. A pile with free head support reaches its maximum lateral capacity when one plastic hinge is formed, while piles with fixed supported heads have higher lateral capacity since two plastic hinges are needed to make the pile becoming a mechanism.

2.3.1 Lateral capacity calculation

Figure 2.1 illustrates the behaviour of a laterally loaded pile embedded in cohesive soil, a theory developed by Broms (1964a). The lateral capacity for a free head pile is found in Davies and Budhu (1986) given as follows:

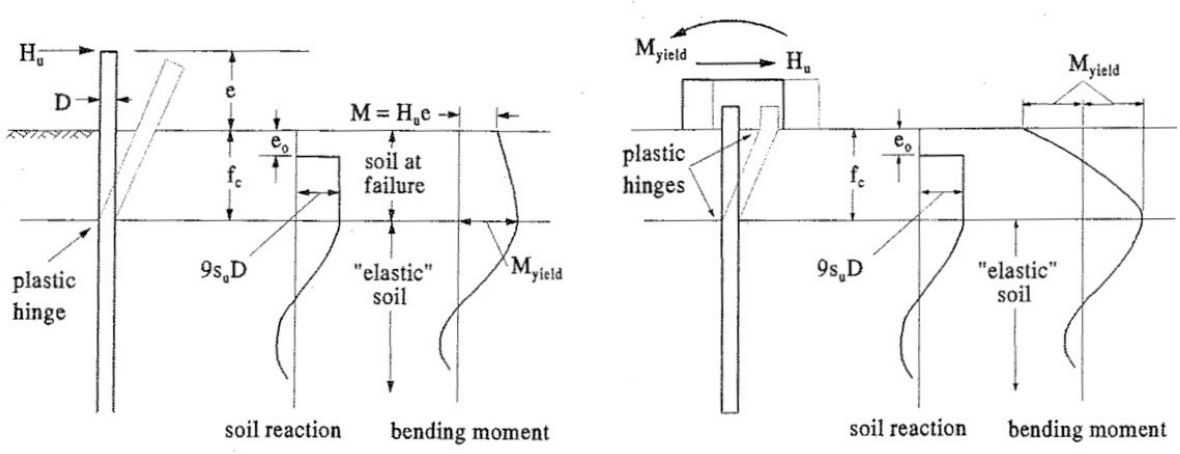

Figure 2.1: Pile-soil interaction for cohesive soil, a) free head and b) fixed head pile (Broms (1964a)).

$$H_{\mathrm{u}} = s_{\mathrm{u}} D^2 \left[(2n_{\mathrm{c}} + 100f^2)^{0,5} - 10f \right] \tag{8}$$

where s_u is the undrained shear strength of the soil, D is the pile diameter, f is the eccentricity for expressing the resulting pile head moment; n_c is a ratio expressed as:

$$n_{\mathrm{c}} = \frac{10 M_{\mathrm{y}}}{s_{\mathrm{u}} D^3} \tag{9}$$

The yielding moment occurs at the location given by:

$$f_{\mathrm{c}} = \frac{H_{\mathrm{u}}}{9 s_{\mathrm{u}} D} + e_0 \tag{10}$$

where $9s_uD$ is the pressure bellow e_0. e_0 is a defined depth below the ground surface, equals 1,5 pile diameters, where the soil does not contribute to the pile-soil interaction. The assumption of no stabilizing effect from the soil above e_0 is found in the article by Broms. This is justified because the soil stiffness near the ground surface is varying (Broms (1964a)). Davies and Budhu (1986) has set the depth e_0 to 0,6 meters in their research paper. Pile heads which are fixed supported has a ultimate lateral capacity of:

$$H_{\mathrm{u}} = 2s_{\mathrm{u}}D^2{n_{\mathrm{c}}}^{0,5} \tag{11}$$

2.4 Winkler Foundation Modeling

Jia (2018) describes Winkler foundation modelling as an ultimate load method, i.e., simplification of the soil behaviour by using load-deflection curves at each representative depth. To manage this, the pile-soil structure is discretely divided into some parts, where the interaction between the soil and the pile is described through the implementation of nonlinear springs. The springs are uncoupled and carry loads between the pile and the surrounding soil at every defined depth. To define the spring properties, the p-y curve is a widespread alternative, which is the subject for section 2.5.

2.5 Lateral Force-Displacement of piles: p-y curve

Since piles resist lateral loads through shear, bending, and earth passive resistance, the capacity to handle this load type depends on the pile stiffness, soil type, soil stiffness, and whether the pile head is fixed or free (Helwany (2007)). As mentioned in section 2.4, one method to define the Winkler springs resistance properties is to use the p-y curve. The p-y curve method was made by McClelland et al. (1956) and further developed by Reese et al. (1975) and is able to describe many different cases, e.g. inhomogeneous soil types, layered soils, nonlinear soil behaviour, different pile materials and cross-sections (Jia (2018)).

According to Jia (2018) modeling piles surrounded by soils and exposed to horizontal loading could be done through the following equilibrium equation:

$$EI\frac{d^4y}{dz^4} + N\frac{d^2y}{dz^2} + p + q = 0 \tag{12}$$

where y is the lateral deflection at depth z meters underneath the ground surface; EI is the bending stiffness of the pile; N is the axial force in the pile; p = -E_sy is the soil reaction per unit length; E_s is the secant modulus of soil reaction. Equation (12) needs to define the boundary conditions for bending moments, M, shear forces, Q, and rotations of the pile, θ, in order to be solved. These are described as:

$$M = -EI\frac{d^4y}{dz^4} \tag{13}$$

$$Q = -\frac{dM}{dz} + N\frac{dy}{dz} \tag{14}$$

$$\theta = \frac{dy}{dz} \tag{15}$$

2.5.1 Calculation of Ultimate Lateral Resistance, p_u

To establish p-y curves, the ultimate lateral resistance, p_u, is required. For clays, the ultimate lateral resistance is coupled to the failure mechanism of the pile. This could either be a wedge failure mechanism or a flow failure mechanism. It is assumed that the wedge failure mechanism occurs nearby the ground surface and that the flow mechanism takes place deeper down (Jia (2018)). To calculate the ultimate resistance per unit length of pile below a depth of 1,5 times the pile diameter Broms (1964) proposes to use the expression:

$$p_u = N_p s_u \tag{16}$$

where N_p is an ultimate resistance coefficient which is non-dimensional and has an upper limit value of 9 as the depth increases; s_u represents the shear strength of clays (Broms (1964)).

Chapter 3

Methodology

The intention of this chapter is to present the method which has been applied for the case study and the analyses. Firstly, the research method is used. Secondly, the applied software SAP2000 is briefly introduced. This section is followed by a description of the modal analysis, which is connected to the next section, which is related to the static pushover curve. The following section describes the applied methods from EC8. Estimation of the horizontal elastic response spectrum, determination of the earthquake load and calculation of the pile stiffness are the headlines in this section.

3.1 Research method

The scientific method is, according to Vining (2013), a research method that starts with a specific problem and seeks to find a theoretical explanation of the occurring phenomenon, i.e. the observed results. Relevant theory is used as a guideline to find a theoretical solution to solve the investigated problem. The next step is to collect relevant data by building models. The models are applied for data analysis, and the results are interpreted to see if the tested solutions solve the investigated problem. The process stops when the researcher finds that the data results confirm the solution. This method is relevant for the experimental tests that the numerical simulations are based on.

The research object intends to discover the impact of allowing the piles to behave plastically. Since there are no physical experimental tests to apply for evaluation of the reliability of the results from the analyses in SAP2000, it is necessary to detect the validity of the results by performing multiple simulations. This because a repetitive development of the results increases the probability for the results to be valid. The analyses are performed multiple times, where only

one parameter is changed for each simulation. These choices in the research method increase the strength of the reliability since this gives an indication of a high degree of accuracy (Grenness (1997)). The performed analyses and calculations are based on established theory, i.e. a deductive method has been applied (Christoffersen and Johannessen (2012)). This contributes to strengthening the validity of the results.

Winsberg (2003) defines computer simulation as a method where a system is inspected systematically. The specific way of doing this is to choose a model, implementing it into a computer program to calculate the output of appropriate algorithms. The output is visualised in the program for investigation by the researcher. The method of simulations differs from simple computations on computers in the way that the results are not always reliable. The literature written by Oberkampf and Roy (2010) tells that the models produced from the scientific method intend to validate the results from computer simulation, i.e. comparing the model output with relevant experimental test results.

3.1.1 Approach

3.2 The analyses in this thesis are conducted by investigating a structure from a chosen case study. The applied loads are identical to the ones applied by the designers that designed the structural support. These loads are given in Appendix A - part 1 of this thesis. To obtain the analyses in this thesis, the system is implemented into a civil-engineering software named SAP2000. This software is described in section 3.2 and the approach related to the setup and implementation of loads is found in section 3.4. The starting point is to run an analysis related to a superstructure supported by pinned supports, given in section 5.1. This is done in order to investigate whether the superstructure itself obtains realistic behaviour. Next, the same superstructure is analysed with linear springs with applied stiffness as described in section 33. To investigate if bi-linear properties of the pile system are implemented correctly, two of the linear piles are replaced with bi-linear piles. If the pushover curves of the linear pile supports and system with both linear and bi-linear supports are identical until the point of yielding, the bi-linear behaviour is assumed to be implemented. This leads to the investigation of bi-linear piles, which is conducted through a parameter study.

3.2 SAP2000

In order to analyse the superstructure, computer software SAP2000 is applied. The software manual describes this to be a general-purpose civil-engineering software which enables, e.g. detection of structural response to earthquake loading. The seismic load generation and distribution follow code-based guidelines, where the results are shown both visually and as plotted graphs. Modal and nonlinear pushover analyses are embedded in the software and found relevant for the work to investigate the superstructure (CSI (2019)). These analyses and their purposes are further described in the next sections.

3.3 Modal analysis

The natural dynamic characteristics of a system, i.e. the natural frequencies, damping factors and mode shapes, are according to Fu and He (2001) described mathematically through a method called the modal analysis. This method is based on linear behaviour of the examined structure. The reference manual for SAP2000 informs that the primary concern of the modal analysis is the lateral displacement of the system. Also, the natural frequency, found by the application of eigenvector analysis, is of interest because this labels the frequencies of dynamic loads where resonance is expected to happen (CSI (2019)). The modal analysis is done as a preparatory dynamic analysis of the superstructure, as a contribution to performing greater comprehension of the structural behaviour. Further, the mode shape obtained from the modal analysis is applied to determine the load distribution in the pushover analysis.

3.4 Static-pushover analysis

Eurocode 8 propose pushover analysis, among others, for verification of the structural response to seismic actions (EN et al. (2004)). Static pushover analysis is according to the reference manual for SAP2000 aiming to find the ultimate load condition of the inspected structure. The structure gets exposed to gravity loading and a monotonic displacement-controlled lateral load pattern. These loads increase continuously, making the structure behave inelastically at maximum loading. The load pattern is representing the base shear from seismic loads and shaped based on the mode shape found in the modal analysis, which is described in the above section. A static-pushover curve is the output from the analysis and describes the ductile capacity of the structure. The parameters shown in this graph is bending moment against rotation or force against displacements, i.e. base shear versus roof displacement (CSI (2019)).

Table 3.1: Seismic Importance Factor from NS-EN 1998-1, NA.4(901) (Standard (2004)).

Seismic Importance Class	γ_1 values
I	0,7
II	1,0
III	1,4
IV	2,0

3.5 Eurocode 8

The purpose of the Eurocode 8 is to design a system capable of withstanding an earthquake without collapsing. This standard consists of six parts, where part 1 and 5 are the parts applied in this thesis. This section gives a description of the horizontal elastic response spectrum, determination of applied earthquake load and calculation of the pile-head static stiffness.

3.5.1 Horizontal elastic response spectrum

The horizontal elastic response spectrum is applied for describing the ground motion of an earthquake for every period, T. In order to identify the magnitude of the horizontal elastic response spectrum, the design ground acceleration has to be calculated by equation:

$$a_{\mathrm{g}} = \gamma_1 a_{\mathrm{gR}} \tag{17}$$

where a_{gR} is the reference ground acceleration of A type soil, γ_1 is the importance factor, with values as given in Table 3.1 and defined based on the seismic importance class given in Table NA.4(902) in EC8, part 1. Determination of the reference ground acceleration is done through application of Appendix A1, point NA.3.2.1. This figure is a map showing the lower part of Norway and corresponding horizontal spectral acceleration at the bed rock for undamped natural frequency of 40 Hz for 5 percent damping ratio, i.e. a_{g40Hz}, with a return period of 475 years. Further, the reference ground acceleration, a_{gR}, is set to be:

$$a_{\mathrm{gR}} = 0,8 a_{\mathrm{g40Hz}} \tag{18}$$

This result is applied in equation 17. In EC8 Part 1, Norwegian Annex, Table NA. 3.1, the soil groups are categorized in the groups A, B, C, D, E, S_1 and S_2. The parameters to describe the horizontal elastic response spectrum are found in Table 3.2. These parameters are further applied to describe the horizontal components of the seismic load. This is shown in the elastic

Table 3.2: Recommended parameters for the elastic response spectrum (Standard (2004)).

Soil type	S	T_{B} (s)	T_{C} (s)	T_{D} (s)
A	1,00	0,10	0,25	1,7
B	1,30	0,10	0,30	1,5
C	1,40	0,15	0,30	1,5
D	1,55	0,15	0,40	1,6
E	1,30	0,10	0,30	1,4

response spectrum, which is given by the following expressions:

$$0 \leq T \leq T_{\mathrm{B}}: \qquad S_{\mathrm{e}}(T) = a_{\mathrm{g}} S \left[1 + \frac{T}{T_{\mathrm{B}}}(2,5\eta - 1)\right] \tag{19}$$

$$T_{\mathrm{B}} \leq T \leq T_{\mathrm{C}}: \qquad S_{\mathrm{e}}(T) = a_{\mathrm{g}} S 2,5\eta \tag{20}$$

$$T_{\mathrm{C}} \leq T \leq T_{\mathrm{D}}: \qquad S_{\mathrm{e}}(T) = a_{\mathrm{g}} S 2,5\eta \left[\frac{T_{\mathrm{C}}}{T}\right] \tag{21}$$

$$T_{\mathrm{D}} \leq T \leq 4s: \qquad S_{\mathrm{e}}(T) = a_{\mathrm{g}} S 2,5\eta \left[\frac{T_{\mathrm{C}} T_{\mathrm{D}}}{T}\right] \tag{22}$$

where $S_{\mathrm{e}}(T)$ is the horizontal components of the seismic load, T is the natural vibration period of a linear SDOF system, a_{g} is the design ground acceleration on type A ground, S is the soil factor, η is the damping correction factor with a reference value of η = 1,0 for fem percent viscous damping.

3.5.2 Determination of applied earthquake load

The modified capacity spectrum method is an approach to compare the structural behaviour with the response spectrum. This method is described in appendix B of the Norwegian standard NS-EN 1998-1-1, and consists of five steps. In order to perform this comparison, systems with multiple degrees of freedom (MDOF) are transferred to a single degree of freedom (SDOF) systems (Standard (2004)). Firstly, the relationship between the normalized lateral load and the corresponding displacement is given through:

$$\bar{F}_{\mathrm{i}} = m_{\mathrm{i}} \Phi_{\mathrm{i}} \tag{23}$$

where $\overline{\mathrm{F}}_{\mathrm{i}}$ is the normalized lateral force, m_{i} represents the mass of the i-th floor and Φ_{i} describes the normalized horizontal displacement at story i found from the modal analysis. In order to normalize the displacement, Φ_{n}=1 at the roof floor which makes equation 23 become $\overline{\mathrm{F}}_{\mathrm{n}}$ = m_{n} at this checkpoint.

Secondly, the base shear force, F_{b}, and the horizontal displacement at the roof displacement, d_{n}, from the pushover analysis are divided with the modal expansion factor. This is done to expand the displacement to an equivalent a SDOF system. This is according to theory from Chopra (2017), where natural mode shapes are defined to be vectors which behave independently from each other. Through the application of modal expansion, Chopra expresses that all of these independent vectors could be applied as a basis to represent any of the other natural modes (Chopra (2017)). In NS-EN 1998-1-1, the modal expansion is done to expand the MDOF system to a SDOF system through the participation factor. The participation factor is defined by:

$$\Gamma = \frac{m^*}{\Sigma m_{\mathrm{i}} \Phi_{\mathrm{i}}{}^2} = \frac{\Sigma m_{\mathrm{i}} \Phi_{\mathrm{i}}}{\Sigma m_{\mathrm{i}} \Phi_{\mathrm{i}}{}^2} \tag{24}$$

where m^* is the mass of the system with one degree of freedom, defined as $\Sigma m_{\mathrm{i}} \Phi_{\mathrm{i}}$. The base shear of the equivalent SDOF system is expressed as:

$$F^* = \frac{F_{\mathrm{b}}}{\Gamma} \tag{25}$$

which makes the SFOD system respond with a displacement at the roof, given by:

$$d^* = \frac{d_{\mathrm{n}}}{\Gamma} \tag{26}$$

The next part of the modified capacity spectrum method is to determine the idealized perfect elasto-plastic force-displacement relationship, illustrated in Figure 3.1. To calculate the yield displacement, the following expression is suggested:

$$d_y^* = 2\left(d_m^* - \frac{{E_{\mathrm{m}}}^*}{F_y^*}\right) \tag{27}$$

where d_{m} is the displacement which causes the structure to become a mechanism and E_{m} is the energy needed to reach this point.

Together with the mass of the SDOF system and the yield force, the yield displacement from equation 27 is applied for calculation of the period for the equivalent SDOF system, as follows:

$$T^* = 2\pi\sqrt{\frac{m^* d_y^*}{F_y^*}} \tag{28}$$

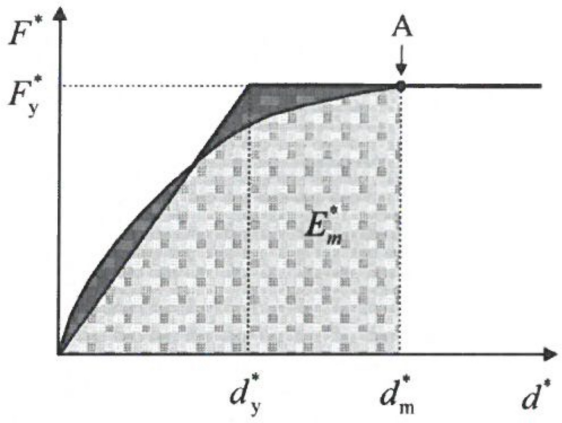

Figure 3.1: Determination of idealized perfect elasto-plastic force-displacement relationship (Standard (2004)).

Table 3.3: Parameters for soil type E to define the elastic response spectrum, type 2 (Standard (2004)).

Type of soil	S (g)	T_{B}	T_{C}	T_{D}
E	1,6	0,05	0,25	1,2

Finally, the maximum displacement to be evaluated is found. This implies finding the displacement at the period T^* of the equivalent SDOF system with unlimited elastic behaviour, d_{et}, given by:

$$d_{\mathrm{et}}{}^* = S_e(T^*)\left[\frac{T^*}{2\pi}\right]^2 \tag{29}$$

where $S_e(T^*)$ is the elastic acceleration response-spectre at the period T^* found through the application of equation 19 to 22, depending on which of these validity areas the period belongs to. The period is categorized from short, medium-long and long length. Short periods are defined as $T^* < T_{\mathrm{C}}$. T_{C} is a threshold value from the elastic acceleration response-spectre, found in table 3.2 and 3.3 in Eurocode 8, part 1. The acceleration response-spectre is given values based on the ground type of the soil, from A to E. For the case study chosen for this thesis, the soil type belongs to category E. The parameters which describe the elastic response spectrum to soil type E is given in Figure 3.3.

The the threshold value T_{C} is illustrated in Figure 3.2. The target displacement for short periods with elastic response, i.e. $F_{\mathrm{y}}{}^* / m^* \geq \mathrm{S_e}(\mathrm{T}^*)$, is defined as $d_{\mathrm{t}}{}^* = d_{\mathrm{et}}{}^*$.

If $F_{\mathrm{y}}{}^* / m^* < S_{\mathrm{e}}(T^*)$ the response is set to be non-linear where the target displacement is yielded by:

$$d_{\mathrm{t}}{}^* = \frac{d_{\mathrm{et}}{}^*}{q_{\mathrm{u}}}\left(1 + (q_{\mathrm{u}} - 1)\frac{T_{\mathrm{C}}}{T^*}\right) \geq d_{\mathrm{et}}{}^* \tag{30}$$

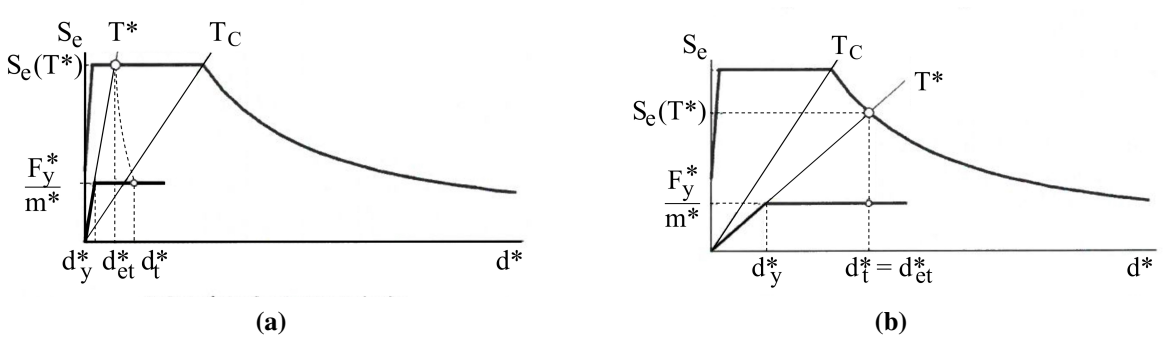

Figure 3.2: Illustration of method to find the target displacement for a equivalent SDOF system with (a) a short period and (b) a medium to long period (Standard (2004)).

where q_{u} is the relationship between the acceleration in a structure with unlimited elastic behavior, $S_{\mathrm{e}}(T^*)$, and the acceleration in a structure with limited strength, $F_{\mathrm{y}}{}^*$ / m^*. This relationship is given by:

$$q_{\mathrm{u}} = \frac{S_{\mathrm{e}}(T^*)m^*}{F_{\mathrm{y}}{}^*} \tag{31}$$

Medium-long periods are defined as $T^* \geq T_{\mathrm{C}}$, illustrated in Figure 3.2 (b), the target displacement is defined as:

$$d_{\mathrm{t}}{}^* = d_{\mathrm{et}}{}^* \tag{32}$$

Once the target displacement is calculated, the modal expansion factor is multiplied with the target displacement in order to give the value of the target displacement for the original MDOF system. Further, the reaction forces from this applied displacement are checked against the capacity of the pile, as given in section 2.3.

3.5.3 Pile-head static stiffness

In Eurocode 8 part 5, NS-EN 1998-5, Annex C Table C.1, the horizontal static stiffness of flexible piles embedded in soil with continuous strength with depth is given (EN et al. (2004)):

$$K_{\mathrm{HH}} = 1,08\left(\frac{E_{\mathrm{p}}}{E_{\mathrm{s}}}\right)^{0,21} dE_{\mathrm{s}} \tag{33}$$

where E_{p} is the Young's modulus of the pile materal, E_{p} is the Young's modulus of the soil, d is the pile diameter. This stiffness is used for the linear spring properties in SAP2000, representing the pile.

Chapter 4

Case study

A case study has been carried out in order to examine the importance of inelastic behaviour of pile foundations. The background of the case study is briefly described at the beginning of this chapter. Thereafter, a description of the investigated system is given. The setup of the investigated system into the SAP2000 software is the topic for the next section. The two final sections are related to the applied load and the calculation of the response spectrum related to the case study.

4.1 Background

The case study is of an apartment building located in Lørenskog. Pictures of the construction site and the floor plan are shown in Figure 4.1. This project is under construction, and the civil engineering team at Consisu has therefore determined all the dimensions and geometry. The building has six stories, which consists of concrete slabs with 250-millimetre thickness supported by steel column and shear walls which are 200 millimetres thick. In order to analyze more aspects of the seismic pile design, the case study is narrowed on one of the shear walls and its supporting piles, see Figure 4.1.

4.2 Investigated system

The shear wall is a continuous shell element retained with the floor at every story of the building. The wall also continues along the with, except from two doors located in the basement. The superstructure is supported on piles at four points, as illustrated in Figure 4.2 (a). The concrete quality for the walls is B35, and the concrete cover above the reinforcement is 25 millimetres. The applied rebar has a diameter of 10 millimetres, consists of four layers and has a spacing

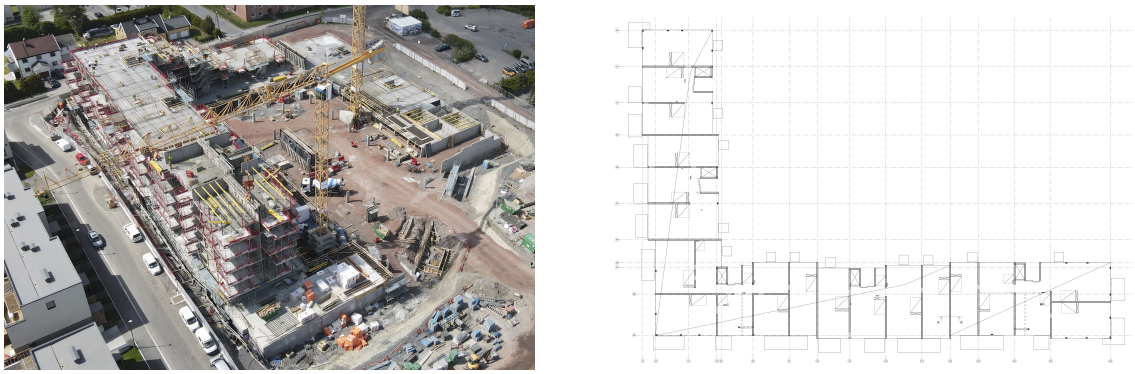

(a) (b)

Figure 4.1: Figure (a) is a picture of the construction site; Figure (b) shows the general floor plan.

of 250 millimetres in both horizontal and vertical direction, as shown in Figure 4.2 (b). The foundation floor has a 400-millimetre thickness and is connected to four piles. These piles are made circular steel cross-sections with both 150 and 130 millimetres in diameter. The soil consists of clay with continuous soil stiffness with depth.

4.3 Setup of the system in SAP2000

Analyzes of the shear wall and the four associated piles are done through SAP2000. The setup of the model is essential in order to make the system behave realistically. In this section, the setup of the superstructure, elastic and bi-linear piles is described in detail.

4.3.1 Superstructure

It was found that the wall had to be divided into squares in the software in order to give a correct location to the piles, where these only could be located at the corners of a square element. Another finding during the modelling process is a need for dividing the squares to join the corners in common nodes which makes the elements interact as one element. The nodes are connected through joint constraints, where diaphragms are given to every node except the base nodes. This gives the superstructure, which is illustrated in Figure 4.5 The materials applied in the model are given nonlinear material properties to enable investigation of the inelastic range. The out of plane displacement is not included in the modal and pushover analysis. The only floor included in the model is the basement floor which is drawn as a beam with a height of 0,4 meters and a with of five meters.

It is essential to define the material properties properly in order to perform analyzes which

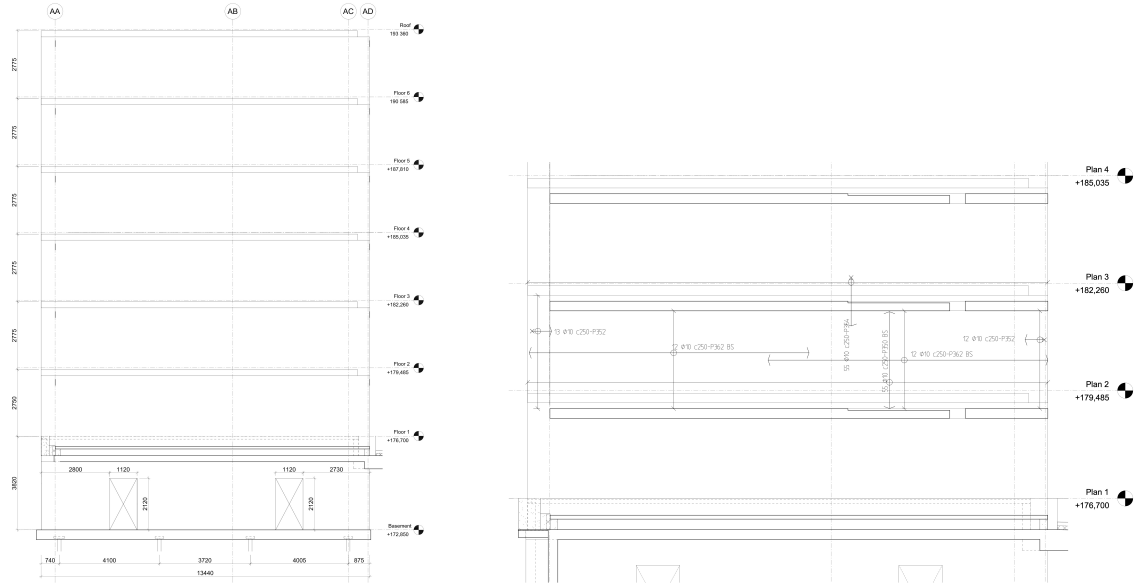

(a) **(b)**

Figure 4.2: Figure (a) is the elevation of the inspected shear wall; Figure (b) illustrates how the reinforcement is structured.

renders the realistic behaviour of the system. The concrete is given a compressive strength of 27,58 MPa and a modulus of elasticity of 37231,69 MPa. The weight per unite volume is 23,56 kN/m^3. The reinforcement is defined for a modulus of elasticity of 200 000 MPa. The applied reinforcement has a diameter of 10 millimetres, a spacing of 250 millimetres in both directions and consist of four layers in total. The nonlinear properties for both the concrete and steel materials are given in Appendix B. The material properties are implemented in the model through a defined area section. This area section is applied when drawing the model in SAP2000. Using the ”Shell-Layered/Nonlinear” to describe the type of area section, the concrete wall is divided into four layers. The first layer is 200 millimetre of concrete, given membrane behaviour. The nonlinear behaviour is defined to appear in direction 2, where the direction is defined in Figure 4.3. The two layers of horizontal reinforcement are omitted from the area section since the shear behaviour is assumed to be elastic. For the vertical reinforcement, these are defined separately with membrane behaviour and a material angle of 90°. This material is defined with nonlinear properties in direction 1. The basement floor has a 400-millimetre thickness and is modelled as a concrete beam with a 5000-millimetre width, where both the concrete and the reinforcement material are inserted to define the behaviour of this structural part.

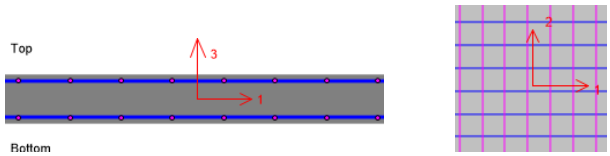

(a) (b)

Figure 4.3: Illustration of the defined concrete area section in SAP2000 and applied direction numbering.

4.3.2 Elastic piles

The elastic piles are modelled by supporting the superstructure by roller supports and springs with horizontal stiffness only. This makes the structure able to move mainly in the horizontal direction. The horizontal spring stiffness K_{HH} are calculated in equation 33 to be 15636,70 kN/m, where the Young's modulus of the pile E_{p} is equal 210 000 MPa. This value is chosen a result of that the pile is made of steel. The pile diameter is 130 millimetres, and Young's modulus of the soil E_{s} is 15 MPa. According to Chopra (2017), elastic properties are described according to Figure 4.4. This figure illustrates that the stiffness k corresponds to the slope of the force-displacement curve. This means that the higher the slope, the higher the force has to be in order to obtain a given displacement. Therefore, the degree of stiffness determines the amount of displacement that appears as a result of exposing the system to a given force. The monitored displacement magnitude of the pushover curve in SAP200 was set to 402,5 millimetre for this system, in order to detect the changes which happen between every step. The minimum number of saved states was set to 400, and the maximum number is set to 1000.

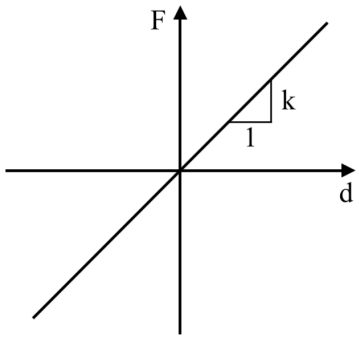

Figure 4.4: Description of the elastic spring behaviour.

4.3.3 Bi-linear piles

Just as the elastic piles, the inelastic piles are modelled by supporting the superstructure by roller supports and springs with horizontal stiffness. The difference is that the spring gets perfect elastoplastic properties, as shown in Figure 4.6. The superstructure with horizontal elastic

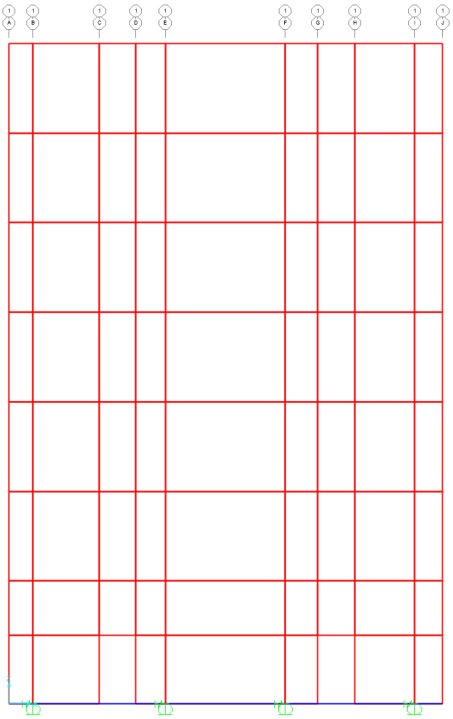

Figure 4.5: Superstructure supported by rollers and springs.

spring support is used as a reference model in order to determine a sensible elastic limit for the multilinear spring. The reaction forces achieved when the roof gets an offset equal to the target displacement from section 3.5.2 is set as the maximum horizontal capacity. Similarly, the displacement limit is the displacement of the basement when the target displacement of the roof is reached. In the SAP2000 user manual, a tool named *link/support element* is pointed out for the implementation of multilinear elastic spring properties into the model. This support element attaches the joints it is mounted on to the ground and is given perfectly plastic behaviour, i.e., no stiffness when the spring reaches its limit (CSI (2019)). To perform pushover analysis with a high degree of accuracy, the number of steps within the investigated displacement is found to be crucial. For the defined load case of the pushover curve, the monitored displacement magnitude was set to 402,5 millimetre for the system supported by both elastic and perfect elastoplastic piles. The superstructure only supported by perfect elastoplastic piles had to be given a lower monitored displacement, i.e. 22,5 millimetre, to register all the points of the pushover curve. As for the elastic piles, the minimum number of saved states was set to 400 states, and the maximum number is 1000.

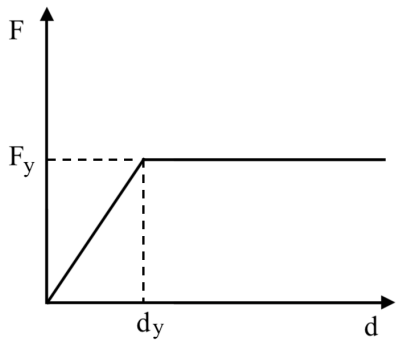

Figure 4.6: Description of the perfect elastoplastic spring behaviour.

4.4 Applied loads

In order to describe the structural behaviour of the superstructure sufficiently, the loads have to be given a reasonable magnitude. Both vertical and horizontal loads appear in the same load case, but for this study, the only horizontal load comes from the seismic event. The dead load from the concrete slabs and the service loads are defined in NS-EN 1991-1-1 Eurocode 1 (Norway (2008a)). The system is also exposed to snow load, which is defined as declared in NS-EN 1991-1-3 Eurocode 1 (Norway (2008b)).

The detected system is a shear wall which gets loads from every floor, 2,5 meters from the centre line of the wall in both directions. The load from this area, are together with the self-load of the wall itself, influencing the natural period of this structural part. Consequently, these loads contribute to the magnitude and distribution of the mode shape from the modal analysis, which is further applied to the pushover analysis. SAP2000 uses *area load* functions to insert the load to shell elements. Therefore, the estimated area loads are firstly divided and transformed to point loads. This is based on the length of the wall area which the load represents. Thereafter, the point loads are divided on the area where the loads are inserted. For the basement floor, the applied loads are implemented as line loads where the load involves a width of five meters. The applied loads in this thesis are given in Appendix A, part 1.

The earthquake is represented by the pushover analysis where the load distribution is taken from the first mode shape, which is defined in SAP2000 through the definition of *load cases*.

4.5 Magnitude of elastic response spectrum

The size of the seismic load is defined by the elastic response spectrum. Through the method described in section 3.5.1, the magnitude of the elastic response spectrum is found. The elastic response spectrum is defined through equation 19 to 22, where the Soil factor, S, and the threshold periods, T_B,T_C and T_D are given in Table 3.2. The design ground acceleration is also a parameter needed to describe the elastic response spectrum. It is calculated as given in equation 17, where γ_1, according to Table 3.1, is set equal 1,0 for structures in importance class II. The reference ground acceleration, a_{gR}, is calculated from equation 18 to be 0,44 m/s^2 for the area which the case study belongs to. The point NA.3.2.1 has been applied to find the undamped natural frequency of 40 Hz for 5 percent damping ratio, a_{g40Hz} which is found to be 0,55 m/s^2. This makes the design ground acceleration, a_g to be 0,44 m/s^2. The estimated elastic response spectrum is given in Figure 4.7.

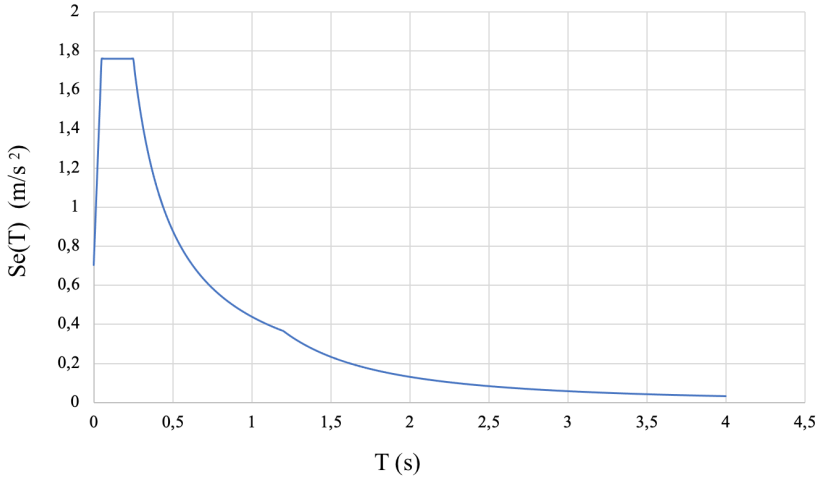

Figure 4.7: The elastic response spectrum for the relevant geographical area.

Chapter 5

Analysis and Results

In the present chapter, analyses of a superstructure with pinned supports are conducted firstly. Thereafter, an identical superstructure with linear piles is examined. This system is applied as a baseline regarding the research objective in this thesis. The reason why this system is applied as a baseline is that EC8 requires that piles should be designed to remain elastic (EN et al. (2004)). The requirement means that the horizontal springs must be given elastic properties which remain throughout the pushover analysis.

5.1 Superstructure with pinned supports

The starting point is to run a modal analysis with pinned supports to find any errors in the SAP2000 model and inspect the natural properties of the superstructure. In this model, there is not any interaction with the pile foundation. A modal analysis is performed to find the natural mode shape, period and frequencies of the structure. Further, a pushover analysis is conducted to detect the applied displacement and coinciding reaction forces.

5.1.1 Modal analysis

As stated in section 3.3, the natural dynamic characteristics of a system are found through the modal analysis. The natural period of the superstructure for the first mode shape is 0,173 seconds, the natural frequency is 5,777 cycles per second, and the mass participation ratio is 0,51. For the third mode, the natural period is 0,053 seconds, and the natural frequency is 18,778 cycles per second. The mass participation ratio is 0,21, which means that this mode contributes less to the total response compared to the first mode naturally. Therefore, the first mode shape is applied to describe the load distribution in the pushover analysis. The distribution is given in Table 5.1 together with the normalized displacement, Φ_i.

Table 5.1: Displacement distribution for Mode shape 1 at every store.

Floor, i	Displacement	Normalized displacement, Φ_i
0	0	0
1	0,227	0,123
2	0,449	0,243
3	0,713	0,386
4	0,999	0,541
5	1,291	0,699
6	1,576	0,854
7	1,846	1.000

5.1.2 Pushover analysis

For the pushover analysis, the material properties have to be defined in the inelastic range, in order to behave properly during the pushover process. The applied load pattern is found through the modal analysis. The first mode, which represents an inverted triangular load distribution, is the one that contributes the most to the structural response and the only one analyzed in the pushover analysis. The pushover analysis in SAP2000 is set to stop when the displacement for the analysis reaches 1,02 meters. This gives a pushover curve, as shown in Figure 5.1. In this figure, the maximum achieved stress before structural failure is 4109,53 kN as a result of a roof displacement of 0,157 meters. The deformed shape and the stress distribution of this system is given in Figure 5.2.

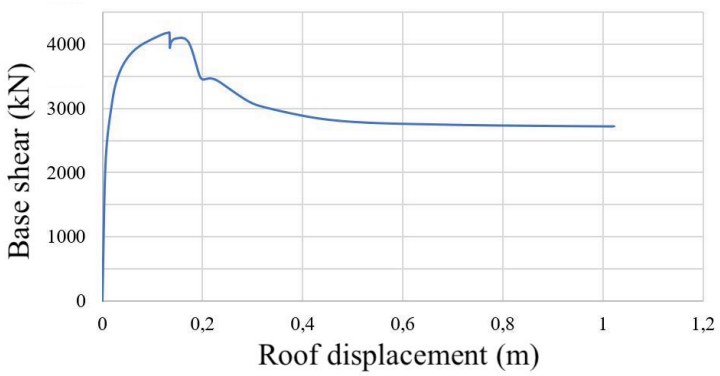

Figure 5.1: Pushover curve for superstructure with pinned supports.

5.1.3 Determination of applied earthquake load

In order to determine the applied earthquake load to the investigated system, the load distribution is using the normalized displacement from the modal analysis, given in Table 5.1. Through

equation 23, applied to every floor and added together, the mass of the equivalent system becomes 321,16 tons. The estimated loads on each floor is given i Appendix A - part 2 of this thesis. This leads to a value of the participation factor of 1,43, from equation 24. Moreover, the pushover curve for the equivalent SDOF system is found through equation 25 and 26. Calculation of the yield displacement is found by equation 27. The applied value of d_{m} is 0,135 meter which is the point where the equivalent SDOF structure becomes a mechanism and the deformation energy which causes this displacement is 356,6 kNm. The yield force F_{y} is set to be the largest force achieved in the pushover curve, i.e. 2939,67 kN. The result is a yield displacement of 0,028 meters. Further the natural period T^* is calculated as given in equation 28, to be 0,36 seconds. Since $T^* \geq T_{\mathrm{C}}$, the period is defined to have medium to long length. This makes the target displacement to be equal to the displacement of a system with unlimited elastic behaviour, which is given by equation 29. The elastic acceleration response-specter $S_e\left(T^*\right)$ at the period $T^* =$ 0,36 seconds 0,36 seconds is 1,23 m/s^2. This period is in a range between T_{C} and T_{D} for the values found in Table 3.3. This indicates that equation 21 should be used for the calculation of the elastic acceleration response-specter at period T^*, where the result is $S_e\left(0,36s\right) =$ 1,23 m/s^2. Thereafter, the target displacement d_t for the SDOF system is calculated according to equation 32, which is found to be 4,0 millimeter. For the original MDOF system, the roof displacement d_n is calculated through $\Gamma d_t =$ 5,67 millimetre. The reaction forces found in the SAP2000 model when the roof displacement is set to 5,67 millimetre is equivalent to 481,99 kN.

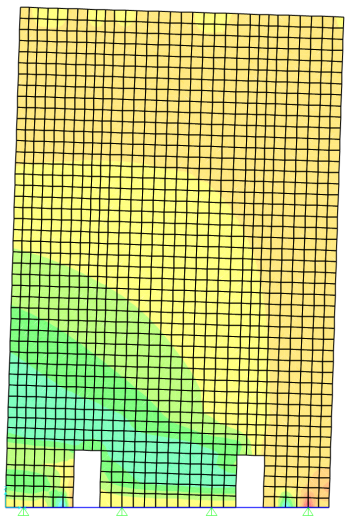

Figure 5.2: Illustration of the deformed shape and the stress distribution for a superstructure with pinned supports; the scale goes from yellow to read for compressive stresses and green to blue colour scale for the tensile stresses.

5.2 Superstructure supported by elastic springs

The piles modelled in this section has linear properties, which is required in EC8. The results found in this section will be the reference points for the cases where the structure is supported by inelastic piles. The pile stiffness is set to be equal, in order to simplify the parameter study in section 5.4.

5.2.1 Modal analysis

The first mode shape achieved for the superstructure supported by elastic springs gets evenly displaced along with the height of the building. It was found that the displacement of the basement and the roof were nearly reaching the same value. This is a result of the springs that provide resistance to horizontal displacement, which are being stretched out. This is illustrated and compared with the pinned structure from section 5.1 in Figure 5.3. The natural period is found to 0,90 seconds. The first mode shape is applied to the pushover analysis. The mode shape for the pinned supported structure is an unfavourable load case and gives the pinned structure a lower capacity than if the superstructure was supported by linear springs. The pinned structure is exposed by a load which has an inverse triangular shape, where the resultant force is located at a higher point above base level than the evenly distributed load. This is illustrated in Figure 5.4.

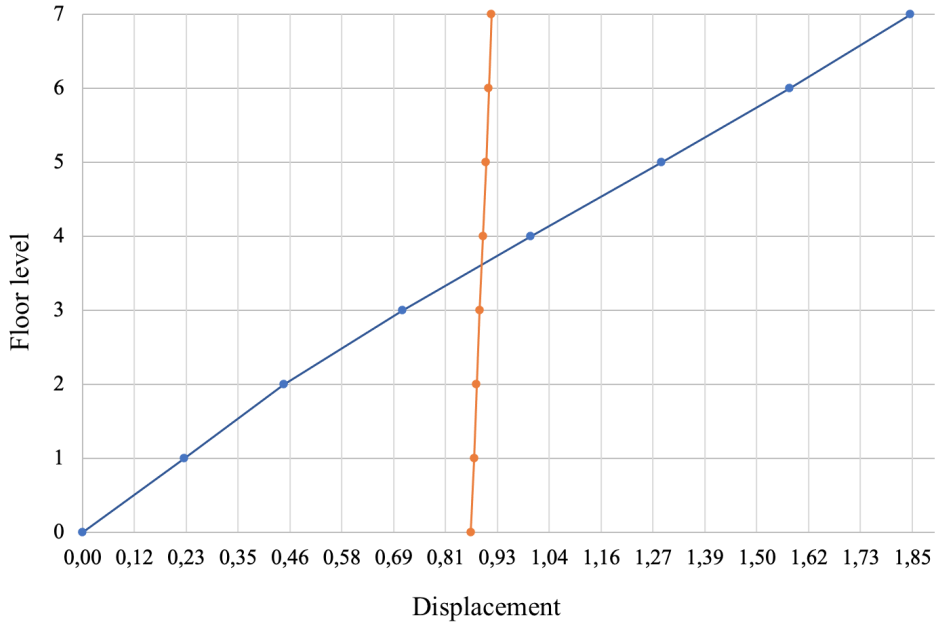

Figure 5.3: Illustration of the first mode shape; Blue curve belongs to the pinned structure; Orange curve is achieved for the structure supported by linear springs.

Table 5.2: Displacement distribution for Mode shape 1 at every store for structure supported by linear springs.

Floor, i	Displacement (mm)	Normalized displacement, Φ_i
0	0,866	0,950
1	0,874	0,958
2	0,879	0,964
3	0,886	0,971
4	0,893	0,979
5	0,9	0,987
6	0,906	0,993
7	0,912	1,000

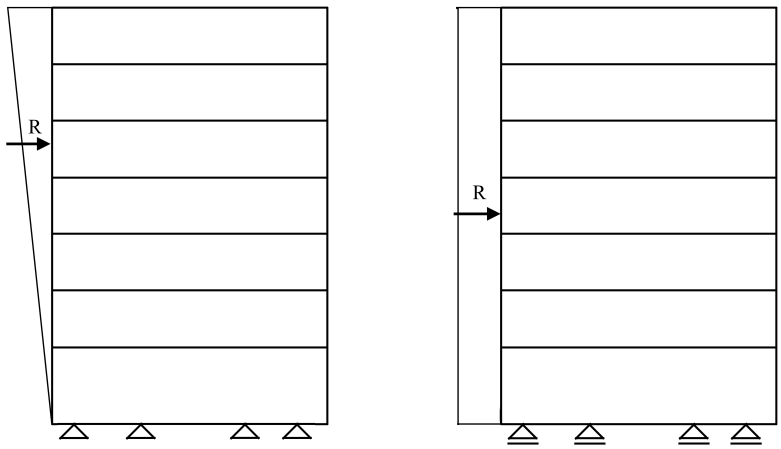

(a) **(b)**

Figure 5.4: Illustration of the load distribution applied in the static pushover analysis.

5.2.2 Pushover analysis

The pushover analysis for the superstructure supported by elastic piles uses the same properties as the pinned supported structure. The superstructure is supported by rollers and linear springs, where the applied load distribution is illustrated in Figure 5.4 b. The result is that the superstructure obtains tensile stresses of 676 N/mm^2 and compression stresses of 603 N/mm^2. The stress distribution and displacement is shown in Figure 5.6. The maximum capacity of this structure is 8688 kN at 256-millimetre displacement. It seems that this system is less stiff and more flexible than the pinned supported structure.

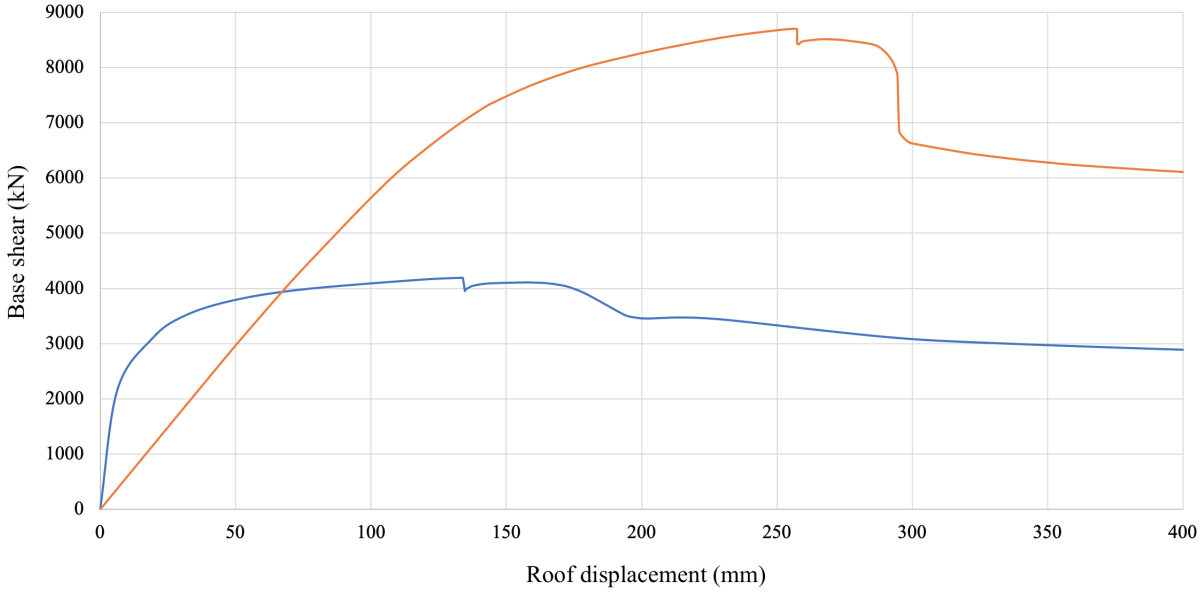

Figure 5.5: Obtained pushover curves, where the blue curve illustrates the pinned structure and orange curve shows the structure supported by linear springs.

5.2.3 Determination of applied earthquake load

The normalized displacement from the modal analysis is applied to find the earthquake load for the superstructure, which is supported by linear springs. Values applied are given in Table 5.2. The mass of the equivalent SDOF system is found through a summation of the result of equation 23, for every floor. The load from each floor is given in Appendix A - part 2. The lumped mass is found to be 696,75 tons, i.e. twice the value of the pinned structure. The calculated parameters described above is applied in equation 24, which gives a participation factor of 1,026. Equation 25 and 26 gives the pushover curve for the equivalent SDOF system. The yield displacement d_y is found to be 0,221 meter by the application of Equation 27. This equation uses the displacement, which makes the system become a mechanism, d_m, which is found to be 0,258 meters by reading the pushover curve for the equivalent SDOF system. The yielding

force is set to be the largest value obtained in the graph, which is 8250 kN. The energy obtained to the point where the system becomes a mechanism is 1653,42 kNm. Equation 28, the period T^* for the SDOF system is calculated to 0,87 seconds. This natural period is within the range of $T^* \geq T_{\mathrm{C}}$, and is therefor defined to have medium to long length. This is according to EC8 part 1, making the target displacement equal the displacement of a system with unlimited elastic behaviour, which is given by equation 29. This period is in a range between T_{C} and T_{D} for the values found in Table 3.3. Hence equation 21 is applied to estimate the elastic acceleration response-spectre at period T^*. Equation 32 is applied in order to find the target displacement d_t for the equivalent SDOF system, which gives a target displacement of 8,84 millimeter. In order to estimate the roof displacement d_n of the MDOF system, the participation factor is multiplied with the target displacement for the equivalent SDOF system, i.e. $d_n = \Gamma d_t = 9{,}07$ millimetre. Reading the pushover curve for this system in Figure 5.5, gives a total base shear of 537,13 kN. This shear force is equally distributed between the piles. This gives a reaction force of 134,28 kN. This equals a base displacement of 8,587 millimetres, using the relationship $F = k \cdot u$ solved with respect to the displacement u. The applied spring stiffness k is 15636,705 kN/m. This reaction force is further applied for the design value which the pile should be capable of handling. The base displacement found is applied to define the behaviour of the springs in SAP2000.

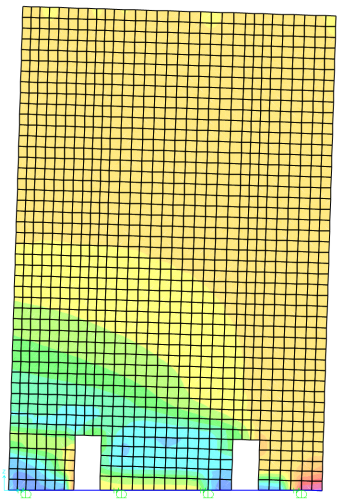

Figure 5.6: Illustration of the deformed shape and the stress distribution for a superstructure supported by linear piles; the scale goes from yellow to red for compressive stresses and green to blue colour scale for the tensile stresses.

5.3 Superstructure supported by linear and bi-linear springs

Which properties to obtain by combining the ordinary design method, i.e. elastic piles, with piles who get inelastic behaviour and permanent deformation is relevant in order to answer the research object of this thesis. These elastic piles are given properties similar to the support system in section 5.2 while the inelastic piles get perfect elastoplastic properties as shown in Figure 4.6. The motivation of this section is to display that the spring properties are implemented correctly. The yielding force is set to 80 $\%$ of the reaction force which the system is designed for, mentioned in the above section. The yielding displacement gets $d_y = 0,8 \cdot d_0 =$ 6,87 millimeter, where $d_0 =$ 8,59 millimeter. At this displacement, the reaction force is 107 kN. Therefore, the pushover curve obtained from section 5.2 should separate from the pushover curve for the system with both elastic and plastic piles when the piles are exposed to this load separately.

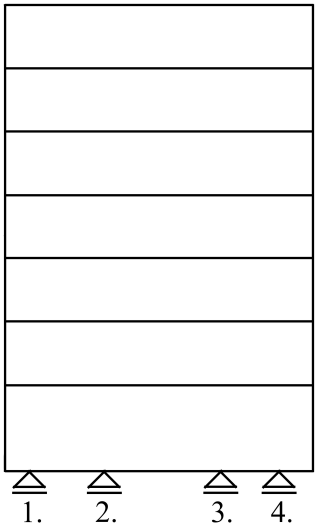

Figure 5.7: Numbering of the supports.

5.3.1 Modal analysis

The modal analysis performed for the system supported horizontally with bi-linear springs shows that the system obtains identical mode shapes as the case where the structure is supported by linear springs. This a result of the initial spring stiffness, which is equal for the two different support systems. Consequently, the natural period and circular frequency are also equal.

5.3.2 Pushover analysis

The horizontal load pattern from the first mode shape, illustrated in Figure 5.3, gives the pushover curve in Figure 5.8, given by the grey-coloured curve. The two curves are identical until the point where the springs at support number 2 and 3 reach maximum capacity. The system in total has a lower capacity than the system supported horizontally by linear springs only. The pushover curve shows that the system reaches a maximum base shear of 7604 kN when the roof displacement is 0,357 meter. The stress distribution of the superstructure which occur as a result of the pushover analysis is given in Figure 5.9. The stresses appear in the reinforcement layer of the SAP2000 model. In this model the tensile stresses are found to be 513 N/mm^2 and the compressive stresses are red to be 167 N/mm^2. These stresses are lower compared to the superstructure supported by linear springs, in section 5.2.

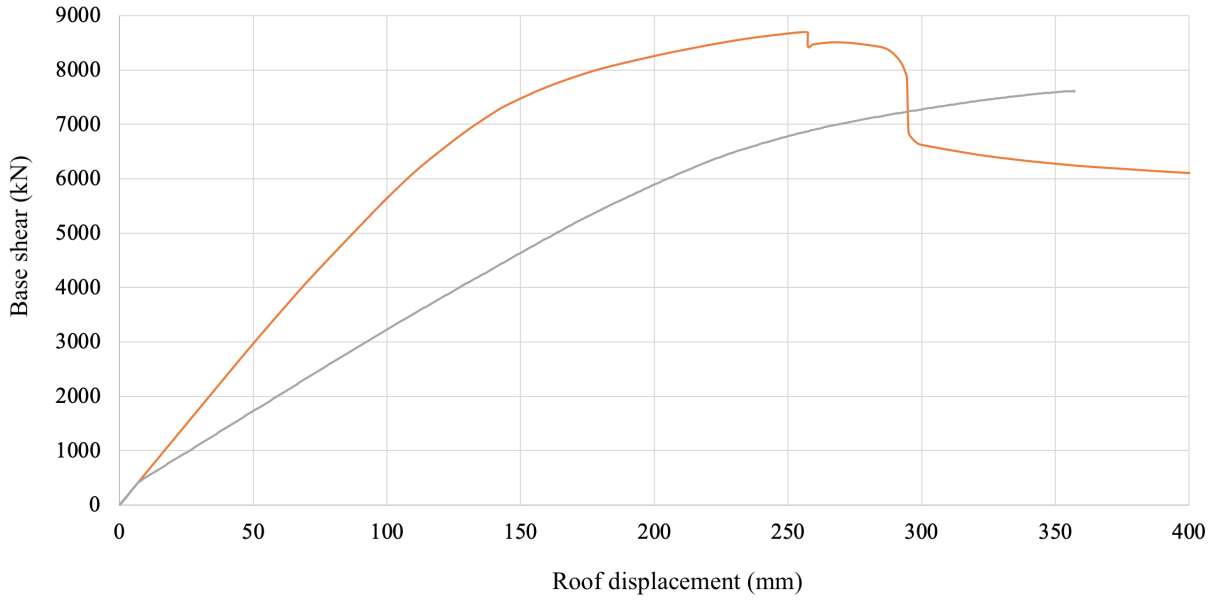

Figure 5.8: Obtained pushover curves; the orange curve represents the system supported by linear springs; the grey curve constitutes the multilinear spring system.

5.3.3 Determination of applied earthquake load

The load distribution from the modal analysis is based on the normalized displacement from Table 5.2, which is identical to the load distribution for the system where linear springs are applied for horizontal stiffness. This makes the lumped mass equal to the results from section 5.2, i.e. 696,75 tons. Also, the participation factor is equal to the superstructure supported by elastic springs which are 1,026. The yield displacement d_y is found to be 0,225 meter by the application of Equation 27. Reading the pushover curve from the equivalent SDOF system,

it is found that the displacement which makes the system become a mechanism, d_{m}, is 0,348 meter. The largest base shear obtained in the pushover curve for the equivalent pushover curve constitutes the yielding force. This force is 7409 kN. The energy obtained to this point is 1644,57 kNm. In equation 28, the period T^* for the SDOF system is calculated to be 0,968 seconds. This natural period is within the range of $T^* \geq T_{\mathrm{C}}$ and defined to have medium to long length. The target displacement for the SDOF system is here equal the displacement of a system with unlimited elastic behaviour, which is given by equation 29. The natural period is in the range between T_{C} and T_{D} from Table 3.3, and uses therefor equation 21 for estimation of the elastic acceleration response-specter at period T^*. The target displacement d_t for the equivalent SDOF system is found to be 10,79 millimeter, using equation 32. This gives a roof displacement of d_n of 11,07 millimetre for the MDOF system, by multiplication of the participation factor with the target displacement for the equivalent SDOF system. The reaction forces from the earthquake, causing a roof displacement of 11,07 millimetre, is 165,81 kN for the linear piles. The piles with bi-linear properties get a reaction force of 107,425 kN since these piles have reached their maximum capacity. The bi-linear piles behave perfectly plastic after reaching a base displacement of 6,87 millimetre, and the reaction force reaches 107,425 kN.

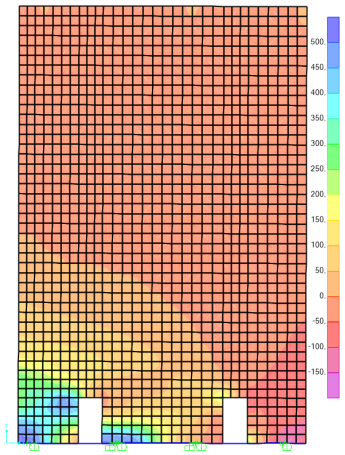

Figure 5.9: Illustration of the deformed shape and the stress distribution for a structure supported by both linear and bi-linear springs; the scale goes from yellow to purple for compressive stresses and green to blue colour scale for the tensile stresses.

5.4 Superstructures supported by perfect elastoplastic piles

In this section, a parameter study of the structural system is conducted, where the horizontal springs have the capacity shown in Table 5.3. The total capacity that is applied as a baseline corresponds to the estimated base shear from the determined earthquake in section 5.2. This

capacity has a value of 537,13 kN and ensures that the systems with perfect elastoplastic piles have sensible and sufficient capacities. The global utilization ratio λ represents the capacity margins. In the parameter study, the applied capacity margins are 30-, 20- and 10 $\%$ above the desired capacity, which corresponds to λ values of 1,3, 1,2, 1,1. Also, a capacity 10 $\%$ bellow what is calculated from the method in EC8 part 1 is included. This gives a global utilization ratio λ of 0,9. The piles are numbered, as shown in Figure 5.7. In the parameter study, every section contains subsections where the capacity of pile 2 and 3 represents the variable parameter. These piles are given the same percentage reduced capacity, represented by the given symbol ι. In total, every section contains the applied reductions ι of 40-, 30-, 20- and 10 $\%$. The reductions are a percentage reduction of the estimated capacity needed for each pile in section 5.2. This capacity is found to be 134,28 kN. The reduced capacity ι causes the outer piles to compensate in order to maintain the global utilization ratio λ, which has been set.

The load distribution from the modal analysis is the same for every variation in this parameter study since the initial stiffness of the perfectly elastoplastic piles are identical. This is done in order to detect the behaviour of the system when the level of elasticity is changed. Utilization ratios, both for the total system and each pile, are calculated for every presented combination of global utilization ratio λ and reduction ι. The ratio is the relationship between the capacity which has been applied and the reaction force that occurs as a result of the earthquake.

In the calculation of the roof displacement, which occurs as a consequence of an earthquake, the calculations are shown in Appendix C. From the calculations in this attachment, it is found that all of the equivalent SDOF systems that belong to the structures supported by perfect elastoplastic piles has a natural period which is categorized to be medium-long. Consequently, the target displacement is equal the elastic displacement, using equation 29 and 32.

Table 5.3: Overview of the section division, based on the capacity margin.

Section	Global utilization ratio, λ	Total capacity (kN)
5.4.1	1,3	698,26
5.4.2	1,2	644,55
5.4.3	1,1	590,84
5.4.4	0,9	483,41

5.4.1 Global utilization ratio λ of 1,3

The first case in this parameter study is a system where the supports are designed with a capacity margin of 30 $\%$ above the desired horizontal capacity of 134,28 kN per pile, found in section 5.2. The capacity margin, in this case, is the highest in this parameter study, which means that this is the most elastic system to be investigated in this parameter study. This section is set up as given in Table 5.4.

Table 5.4: Overview of the subsection division for system where λ is 1,3.

		Capacity (kN)	
Subsection	Reduced capacity of pile 2 and 3, ι ($\%$)	Pile 1 and 4	Pile 2 and 3
5.4.1.1	40	268,56	80,57
5.4.1.2	30	255,13	93,99
5.4.1.3	20	241,71	107,42
5.4.1.4	10	228,28	120,85

5.4.1.1 40 $\%$ reduced capacity of pile 2 and 3, ι

The reduced capacity ι of 40 $\%$ makes the yield force F_y for pile 2, and 3 become 80,57 kN and kept with constant stiffness until the displacement of the base reaches 5,15 millimetre. Similarly, the yield force F_y of pile 1 and 4 are set twice the desired capacity, i.e. 268,56 kN with the same stiffness as pile 2 and 3 until the horizontal displacement of the spring is 17,17 mm. All of the supports are modelled with bi-linear properties. The pushover curve is pictured in Figure 5.10 (a), together with the beginning of the pushover curve from the superstructure horizontally supported by elastic springs. These two curves are identical until the roof displacement reaches 5,2 millimetre, where pile 2 and 3 has reached the perfectly plastic area. From 5,2 to 17,5 millimetre, the pushover curve has a constant slope. Once the structure reaches this point, the curve remains constant at a base shear of 698,26 kN.

The earthquake load is estimated according to the method described in section 3.5.2. The application of the method has been described in detail both in section 5.1 and 5.2. The method is applied in the same matter for this case also. Therefore, the obtained and applied values from this section is given in Appendix C. It is found that the earthquake gives a roof displacement of 8,80 millimetre. This is the target displacement which the system has to resist. From this displacement, the base shear reaches 424,79 kN. The horizontal springs obtain a reaction force of 131,83 kN for pile 1 and 4. These piles are still within their elastic zone, while the springs

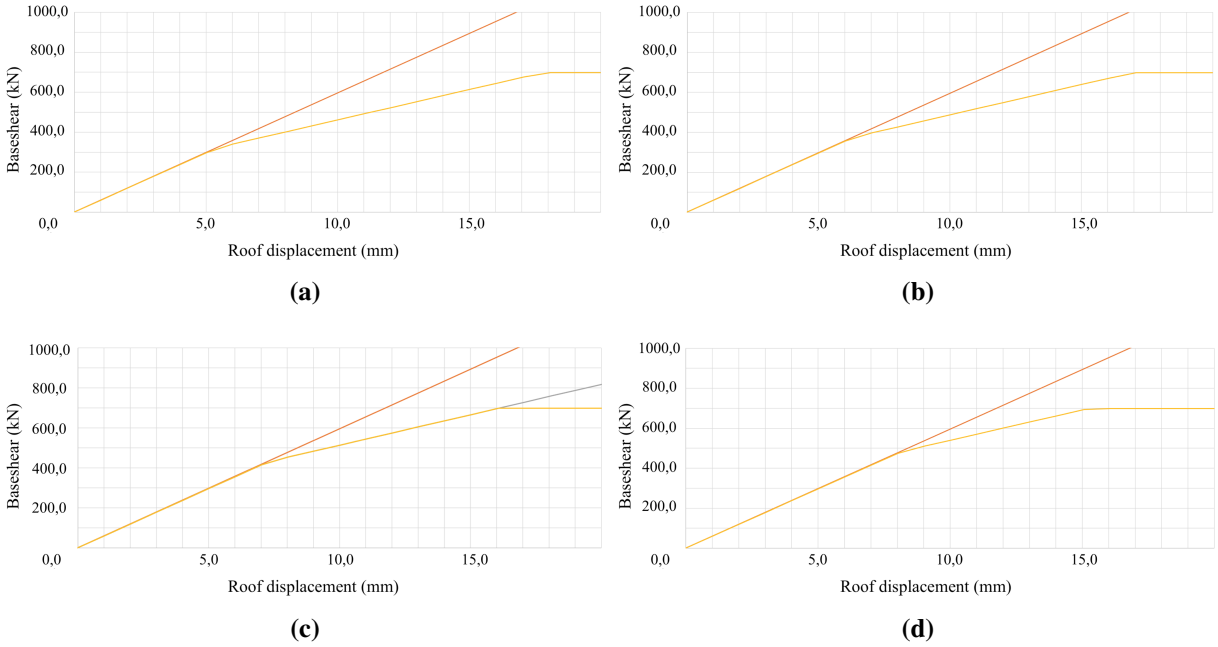

Figure 5.10: Pushover curves where λ is 1,3 and ι is (a) 40-, (b) 30-, (c) 20- and (d) 10 $\%$.

modelled for pile 2 and 3 has reached their maximum capacity of 80,57 kN and has a plastic behaviour at this point, which is shown through a ductility ratio of 1,64 given in table 5.6. The total support system is utilized by a ratio of 0,61. The utilization ratio of pile 1 and 4 is 0,49 $\%$ utilization, and 1,0 for pile 2 and 3 are.

5.4.1.2 30 $\%$ reduced capacity of pile 2 and 3, ι

The yield force F_y for the spring that provides horizontal stiffness for pile 2 and 3 is set to 93,99 kN at a base displacement of 6,01 millimetre. To provide the capacity margin which is being aimed for in this subsection, the lateral working spring has to be kept elastic until F_y reaches 255,13 kN. The displacement which the spring has to be exposed to before entering the perfectly plastic zone is 16,31 millimetre. In Figure 5.10 (b) the capacity of the structure is shown trough the pushover curve. The pushover curve is shown together with the pushover curve for the system with elastic springs, which obtains the same values until spring 2 and 3 are reaching their capacity. From here, the horizontal support is only provided from spring 1 and 4.

The earthquake load that is estimated from the pushover analysis gives a target displacement of the roof of 8,51 millimetre. The calculated values for the estimation of the target displacement are to be found in Appendix C. Reading the pushover curve, the total base shear is 442 kN. This estimated load means that pile 1 and 4 are given a base shear of 127 kN each, while pile 2 and 3 have reached their maximum capacity. Therefore, pile 2 and 3 has a reaction force of 93,99 kN

and given behaviour plastically. Pile 1 and 4 are still within the elastic area. The utilization ratio of pile 1 and 4 are 0,49, and pile 2 and 3 are utilized with a ratio of 1,0. The total utilization ratio of the total support system is 0,63.

5.4.1.3 20 % reduced capacity of pile 2 and 3, ι

The spring properties of pile 2 and 3 are perfect elastoplastic, with a limit F_y of 107,43 kN. These springs have a constant stiffness until the spring is stretched 6,87 millimetre. For pile 1 and 4, the yielding force is 241,71 kN where the pile has been given a displacement of 15,46 millimetre. The pushover curve is shown in Figure 5.10 (c), together with both the structure with elastic springs, from section 5.2, and the superstructure supported by two elastic springs and two bi-linear springs, see section 5.3. The bi-linear springs are given the same properties as pile 2 and 3 in this subsection. Consequently, the pushover curve from this case follows this curve until pile 1 and 4 are reaching their maximum capacity.

The estimated earthquake load gives the structure a roof displacement of 7,95 mm, see Appendix C. The pushover curve gives a base shear of 462 kN. Pile 1 and 4 gets a horizontal reaction force of 123,6 kN while pile 2 and 3 has reached the maximum capacity of 107,43 kN. The outer piles and the piles in the middle are utilized with a ratio of 0,51 and 1,0, respectively. For the support system in total, the utilization of ratio is 0,66.

5.4.1.4 10 % reduced capacity of pile 2 and 3, ι

At a 10 % reduced capacity from the desired horizontal capacity of 134,28 kN per pile, the piles 2 and 3 get plastic behaviour when reaching a reaction force F_y of 120,83. In order to give the support system a total capacity margin of 30 %, the outer piles 1 and 4 are modelled to be kept elastic until each of these piles are exposed to F_y equal 228,27 kN. The spring stiffness of 15636,71 kN/m gives elastic behaviour of spring 1 and 4 until the base displacement reaches 14,59 millimetre. Similarly, pile 2 and 3 has a limit of 7,73 millimetre before the piles are yielding. The pushover curve for this system is shown in Figure 5.10 (d).

The method from section 3.5.2 is applied for the determination of the earthquake load. The calculated key values are given in Appendix C. This method gives a roof displacement of 7,16 millimetre which corresponds to a base shear of 483,4 kN. It is found that all piles contribute equally since none of them is within elastic limit. This gives a reaction force of 120,75 kN per pile. The outer piles, 1 and 4, get a utilization ratio of 0,53 and pile 2 and 3 are utilized by a

ratio of 0,99. It is also found that the total utilization ratio is 0,69.

Table 5.5: Normalized reaction forces and roof displacements from earthquake load when λ is 1,3.

		Normalized force		
ι (%)	d_n (mm)	F1 and F4	F2 and F3	Total
40,0	8,80	0,49	1,0	0,61
30,0	8,51	0,50	1,0	0,63
20,0	8,32	0,51	1,0	0,66
10,0	8,14	0,53	0,99	0,69

Table 5.6: Obtained base displacements and ductility ratio λ is 1,3.

		Normaliced displacement	
ι (%)	d_0 (mm)	D1 and D4	D2 and D3
40,0	8,43	0,49	1,64
30,0	8,12	0,50	1,35
20,0	7,91	0,51	1,15
10,0	7,72	0,53	0,99

Table 5.5 shows the results from this section, which indicates that the roof displacement gets reduced as the difference between the elastic properties between the outer and the middle located piles decreases. This is an effect of the increased stiffness of the support system, which is strengthened as the difference between the capacity of the outer and middle piles in each subsection are reduced. As Table 5.5 gives the utilization ratio of the piles; this does not describe the extent of the plastification. This is given in Table 5.6, where the base displacement and the ductility ratio of each pile are shown. The base displacement is calculated by dividing the largest obtained reaction force on the stiffness of the spring. The largest obtained reaction force is in general found at the outer piles. It is to be assumed that the displacement of the piles are equal, even though their yield capacity and yield displacement are different. The ductility ratio is above 1,0 in every case, except from the situation where the reduced capacity of pile 2 and 3 are 10 %. The ductility ratio is 1,0, which means that the pile is at the threshold value when it comes to elastic behaviour. For the other cases, piles 1 and 3 are beyond their elastic limit and are therefore behaving plastically.

5.4.2 Global utilization ratio λ of 1,2

The global utilization ratio λ applied in this section is 1,2, making the supports less elastic than what has been performed when λ had a value of 1,1. This will participate in detecting how

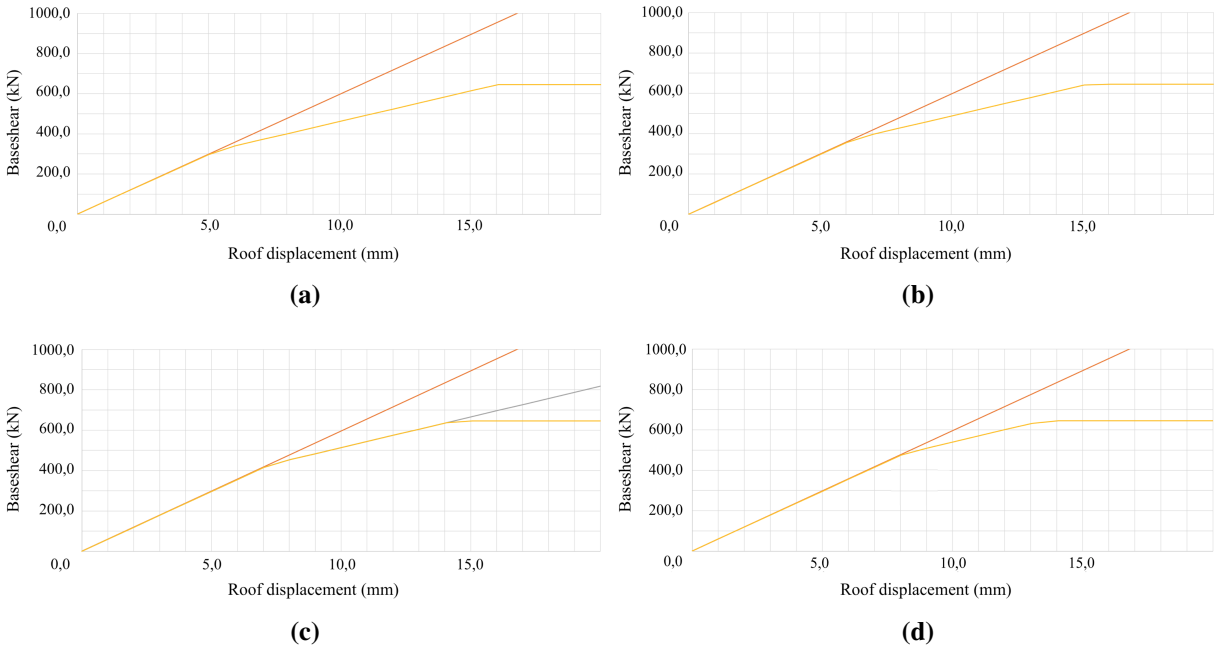

Figure 5.11: Pushover curves where λ is 1,2 and ι is (a) 40-, (b) 30-, (c) 20- and (d) 10 $\%$.

the elasticity affects the structural system. The subsections are divided based on the reduced capacity of the middle located piles. The set up of this part is given in Table 5.7.

Table 5.7: Overview of the subsection division for system when λ is 1,2.

		Capacity (kN)	
Subsection	Reduced capacity of Pile 2 and 3, ι ($\%$)	Pile 1 and 4	Pile 2 and 3
5.4.2.1	40	241,71	80,57
5.4.2.2	30	228,28	94,00
5.4.2.3	20	214,858	107,43
5.4.2.4	10	201,428	120,85

5.4.2.1 40 $\%$ reduced capacity of pile 2 and 3, ι

The applied yield force for the horizontal spring F_y for pile 1 and 4 is 241,71 kN. This is done to achieve a global utilization ratio λ of 1,2, where pile 2 and 3 are given a reduced capacity ι of 40 $\%$. The pushover curve is shown in Figure 5.11 (a). The superstructure with elastic springs and the investigated system in this section follows the same path to the point where pile 2 and 3 get perfectly plastic properties. The whole structure becomes a mechanism when the pushover curve reaches a base shear of 644,55 kN.

Based on the pushover curve, the estimated earthquake load gives a roof displacement of 8,28

millimetre and a total base shear of 420 kN. The applied values for this result is given in Appendix C. The reaction force of pile 1 and 4 is 129,43 kN. This corresponds to a utilization ration of 0,535. The roof displacement, which is presented makes pile 2 and 3 behave perfectly plastic where the utilization ratio has reached 1,0. The total utilization ratio is found to be 0,65.

5.4.2.2 30 % reduced capacity of pile 2 and 3, ι

The capacity margin of 30 % makes the support system capable of handling a base shear of 644,55 kN. Since pile 2 and 3 are given a reduced capacity ι of 30 %, the spring at support 1 and 4 get a capacity of 228,27 kN in the lateral direction. Figure 5.11 (b) shows the pushover curve of the system. This curve shows the capacity of the system and that the system is only is supported by the outer springs when the base shear reaches 375,99 kN, equal 93,99 kN per pile support.

The earthquake load is determined to give a roof displacement of 8,37 millimetre which corresponds to a base shear of 438,10 kN. The outer piles are still kept within the elastic range. For pile number 2 and 3, the limit has been reached and are consequently given plastically properties. Consequently, pile 1 and 4 get a shear force of 125,44 kN each, while each of the piles in the middle gets a lateral reaction force of 93,99 kN. This distribution gives a total utilization ratio of 0,68. The utilization of pile 1 and 4 is of a ratio of 0,55. Pile 2 and 3 have a utilization ratio of 1,0.

5.4.2.3 20 % reduced capacity of pile 2 and 3, ι

The downward adjustment of 20 % for pile 2 and 3, ι, results in a lateral capacity of 107,42 per pile. Pile number 1 and 4 are designed with a capacity of F_y of 214,85 to keep the system within a global utilization ratio of 1,20. These capacities correspond to a displacement of 13,74 millimetre and 6,87 millimetre for the outer piles and middle piles, respectively. These given properties give the superstructure the capacity as shown in the pushover curve in Figure 5.11 (d).

It is found that the earthquake load for a system which obtains a pushover curve as illustrated in Figure 5.11 (c) gets a roof displacement of 8,19 millimetre. Appendix C shows the parameters and sub-calculations, which gave this result. A base shear of 458,76 kN is found to correspond to this displacement, where pile 2 and 3 are deflected to a point where the supports are getting permanent deflection. This corresponds to a utilization ratio of 1,0. Pile 1 and 4 are still having elastic properties, where the reaction force is 121,96 kN the utilization ratio is 0,57. The total

system has a utilization ratio of 0,71.

5.4.2.4 10 % reduced capacity of pile 2 and 3, ι

A global utilization ratio of 1,2 combined with a 10 % reduced capacity of pile 2 and 3, ι, demands a lateral capacity of the outer piles of 201,42 kN. The obtained pushover curve for this system is given in Figure 5.11 (d).

The result from the determination of the earthquake load, described in section 3.5.2, is a roof displacement of 8,02 millimetre. The calculated values are collected in Appendix C. This roof displacement gives a total base shear of 476 kN and is distributed equally between each of the piles. This happens as a consequence of that these are all still kept with properties within the elastic range. Thus, the reaction force is 119 kN. This gives a total utilization ratio of 0,74. This also makes the utilization ratio for the outer and middle piles being 0,59 and 0,985, respectively.

The utilization ratios and roof displacements from this section are collected in Table 5.8. By comparing these results, it is detected that the tendency found from the situation with a capacity margin of 30 % also remains if the capacity margin is reduced additionally by 10%. The intended tendency is that the roof displacement, which occurs as a result of the earthquake load was reduced as a consequence of decreasing the difference between the piles in the outer and in the middle. The ductility ratios are given in Table 5.9, where pile 2 and 3 are given less ductility as their reduced capacity is increased from each subsection. When the capacity of pile 2 and 3 is reduced by 10 %, these piles are still elastic.

Table 5.8: Normalized reaction forces and roof displacements from the earthquake load when λ is 1,2.

		Normalized force		
ι (%)	d_n (mm)	F1 and F4	F2 and F3	Total
40,0	8,67	0,53	1,0	0,65
30,0	8,37	0,55	1,0	0,68
20,0	8,19	0,57	1,0	0,71
10,0	8,02	0,59	0,98	0,74

5.4.3 Global utilization ratio λ of 1,1

The capacity margin of the total support system is decreased further in this section. This part of the parameter study constitutes the lowest investigated capacity margin, where the next section is below the required capacity from EC8. The subsections which belong to this part is set up as

Table 5.9: Obtained base displacements and ductility ratios when λ is 1,2.

		Normaliced displacement	
ι (%)	d_0 (mm)	D1 and D4	D2 and D3
40,0	8,28	0,53	1,61
30,0	7,99	0,55	1,33
20,0	7,80	0,57	1,14
10,0	7,61	0,59	0,98

given in Table 5.10, where the capacity of both the outer and middle piles are described.

Table 5.10: Overview of the subsection division for system with a global utilization ratio, λ, of 1,1.

		Capacity (kN)	
Subsection	Reduced capacity of pile 2 and 3, ι (%)	Pile 1 and 4	Pile 2 and 3
5.4.3.1	40	214,85	80,57
5.4.3.2	30	201,42	93,99
5.4.3.3	20	187,99	107,43
5.4.3.4	10	174,57	120,85

5.4.3.1 40 % reduced capacity of pile 2 and 3, ι

The capacity of the support system with a global utilization ratio λ of 1,1, makes the piles able to handle a base shear of 590 kN before the system gets plastic. Here, the piles 2 and 3 are given a reduced capacity, ι, of 40 % from the design value from section 5.2. As a result, pile 1 and 4 has a yield force F_y of 214,85 kN separately, while pile 2 and 3 has a capacity F_y of 80,57 kN each. The horizontal resistance is modelled as a spring with perfect elastoplastic properties. Thus, the outer piles get a displacement of 13,74 millimetre before reaching the perfectly plastic area, while pile 2 and 3 are kept elastic until the piles get a displacement of 5,15 millimetre. These properties are shown in Figure 5.12 (a).

The earthquake load is determined to cause a roof displacement of 8,52 millimetre and a corresponding base shear from the pushover curve of 415,00 kN. The calculations are to be found in Appendix C. The horizontal spring properties give a distribution of 126,93 kN for pile 1 and 4 while the middle piles are exposed to a shear force of 80,57 kN. The middle piles, with a given number of 2 and 3, have reached the maximum capacity and are having plastic properties and permanent deformation. These piles are therefor having a utilization ratio of 1,0. Pile 1 and 4 has still residual capacity within the elastic range and reaches a utilization ratio of 0,59. In total, the system is utilized with a 0,70 ratio.

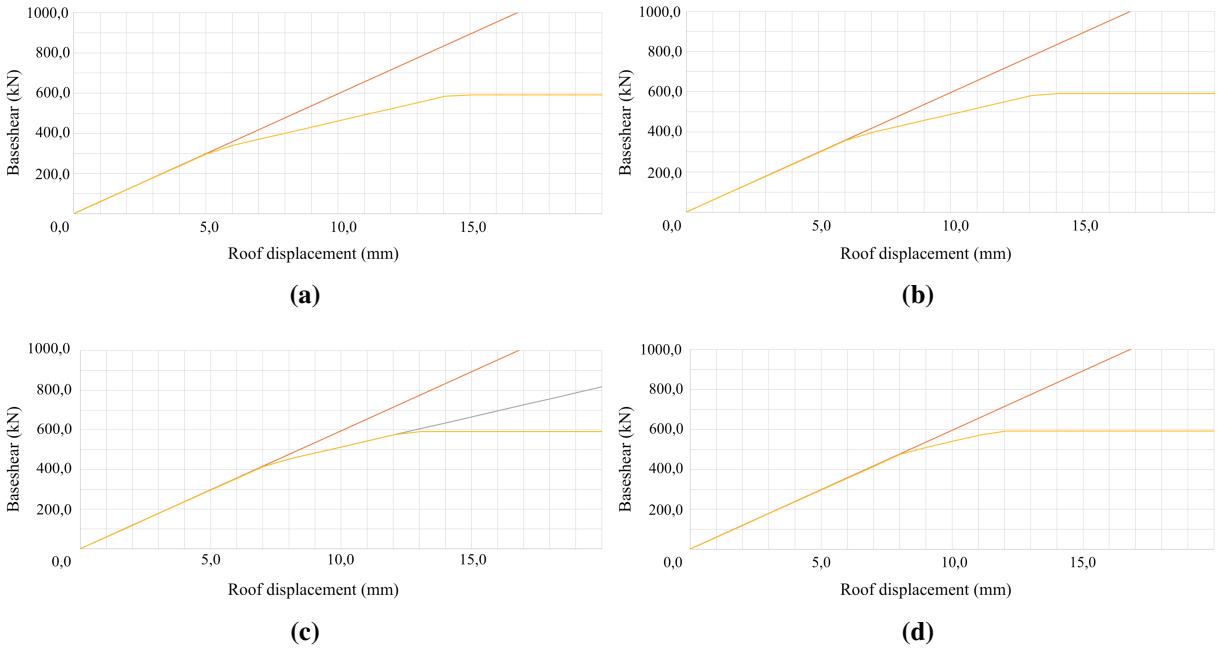

Figure 5.12: Pushover curves where λ is 1,1 and ι is (a) 40-, (b) 30-, (c) 20- and (d) 10 $\%$.

5.4.3.2 30 $\%$ reduced capacity of pile 2 and 3, ι

The outer piles which support the superstructure are given a capacity F_y of 201,42 in order to give the pile system in total a global utilization ratio λ of 1,1, where the condition is that pile 2 and 3 have a 30 $\%$ reduced capacity. The spring stiffness is equal for every horizontal spring in the system and makes the outer piles, i.e. 1 and 4, elastic until the system are given a base displacement of 12,88 millimetre. Equivalently, the middle piles with the given numbers of 2 and 3, behave elastically up to the pile is displaced laterally by 6,01 millimetre. The result of giving the support system properties as presented makes the superstructure behave like illustrated in 5.12 (b).

It is calculated in Appendix c that the outcome of these parameters is an earthquake load which produces a roof displacement of 8,27 millimetre and base shear of 434 kN. The reaction forces at support number 1 and 4 are 123,00 kN per pile, which are within the defined elastic range for the relevant spring properties. These outer piles are utilized with a ratio of 0,61. At the supports located in the middle of the system, the reaction force is at the maximum. Therefore, these springs have been given plastic properties and utilized with a ratio of 1,0. The total utilization ratio of the system is of 0,73.

5.4.3.3 20 % reduced capacity of pile 2 and 3, ι

This part of the parameter study gives a yield force F_y for support number 1 and 4 of 187,99 kN and corresponds to a limit displacement of 12,02 millimetre before the horizontal springs get plastically properties. As shown in Figure 5.12 (c), the pushover curve has the same behaviour as the elastic spring supported superstructure in section 5.2 until the springs at support 2 and 3 reach their elastic limit. Thereafter, the curve follows the pushover curve from section 5.3, illustrated with a grey coloured curve. The pushover curve for this part of the parameter study gets perfectly plastic when the desired capacity is reached.

The roof displacement caused by the estimated earthquake is determined to 8,06 millimetre through the application of the method described in section 3.5.2. The details from this calculation are given in Appendix C. This roof displacement gives a total base shear of 455 kN and a reaction force of 120,10 kN for pile 1 and 4 separately. These piles are kept within the given elastic properties, while pile 2 and 3 behave plastically as a result of the determined earthquake. The utilization of the piles is found to be 0,64 for piles 1 and 4 and 1,00 for pile number 2 and 3. The total system achieves a utilization ratio of 0,77.

5.4.3.4 10 % reduced capacity of pile 2 and 3, ι

The elastic limit for pile number 1 and 4 is 174,56 kN when the base displacement is 11,16 millimetre in this section. The investigated system in this subsection has the smallest difference between the outer piles and those in the middle of all the systems which has a global utilization ratio λ of 1,1. This means that this is the stiffest system within this group. The pushover curve is given in Figure 5.12 (d) and applied to estimate the earthquake load which this system has to be designed for.

The earthquake load is estimated through the calculated values from Appendix C to give a roof displacement of 7,91 millimetre and results in a total base shear of 470 kN. The reaction forces from this earthquake load are 117,50 kN for each pile. This is within the defined elastic properties of all the horizontal springs. The result is that the utilization ratio of the outer piles is 0,67 and 0,97 for pile number 2 and 3. The utilization ratio for the total system is found to be 0,795.

The development that is happening as a result of decreasing the difference between the capacity of the outer piles and the piles in the middle is shown in Table 5.11. This table shows

that the roof displacement is reduced as a consequence of reducing the difference between the capacity of the piles in the middle and the outer piles. By comparing Table 5.5, 5.8 and 5.11, it is observed a reduced roof displacement as a result of decreasing the capacity margin. The ductility ratios in Table 5.12 show the same tendency as Table 5.9 and 5.6, slightly reduced from each equivalent case. The next section investigates the behaviour of the system which are given a total capacity which is 10 % below the required capacity.

Table 5.11: Normalized reaction forces and roof displacements from earthquake load when λ is 1,1.

		Normalized force		
ι (%)	d_n (mm)	F1 and F4	F2 and F3	Total
40,0	8,52	0,59	1,0	0,70
30,0	8,27	0,61	1,0	0,73
20,0	8,06	0,64	1,0	0,77
10,0	7,91	0,67	0,97	0,79

Table 5.12: Obtained base displacements and ductility ratios when λ is 1,1.

		Normaliced displacement	
ι (%)	d_0 (mm)	D1 and D4	D2 and D3
40,0	8,12	0,59	1,58
30,0	7,87	0,61	1,31
20,0	7,68	0,64	1,12
10,0	7,51	0,67	0,97

5.4.4 Global utilization ratio λ of 0,9

The capacity given for the systems in this section corresponds to a global utilization ratio of λ of 0,9. This is the system with the lowest total capacity of all the investigated systems in this conducted parameter study. The total capacity is 10 % below the estimated necessary capacity from section 5.2, with the applied capacities in each subsection as given in Table 5.13.

Table 5.13: Overview of the subsection division for system with a λ value of 0,9.

		Capacity (kN)	
Subsection	Reduced capacity of pile 2 and 3, ι (%)	Pile 1 and 4	Pile 2 and 3
5.4.4.1	40	161,14	80,57
5.4.4.2	30	147,71	93,99
5.4.4.3	20	134,28	107,43
5.4.4.4	10	120,85	120,85

5.4.4.1 40 % reduced capacity of pile 2 and 3, ι

The spring properties in this subsection give an elastic limit of 161,14 kN for pile 1 and 4, which occurs when the piles are given 10,31 millimetre. The result is a pushover curve, as shown in Figure 5.13 (a), where the curve has a constant slope until reaching a base shear of 322,28 kN. The maximum capacity of pile 2 and 3 of 80,57 kN has been reached for this system. Thereafter, the pushover curve gets a reduced slope which continues until the maximum capacity of the system is reached.

The lateral roof displacement that happens as a result of the estimated earthquake is 8,19 millimetre, from Appendix C. By reading the obtained pushover curve in Figure 5.13 (a), it is found that the displacement corresponds to a total base shear of 406,00 kN. This gives a reaction force in support number 1 and 4 of 122,43 kN, which is beneath the elastic limit of the perfect elasto-plastic spring. These outer supports obtains a utilization ratio of 0,76. The supports in the middle, which has a capacity of 80,56 kN, are given permanent deflection as a result of this earthquake load. Thus, the utilization ratio of these spring is 1,0. The total utilization ratio of the support system is 0,84.

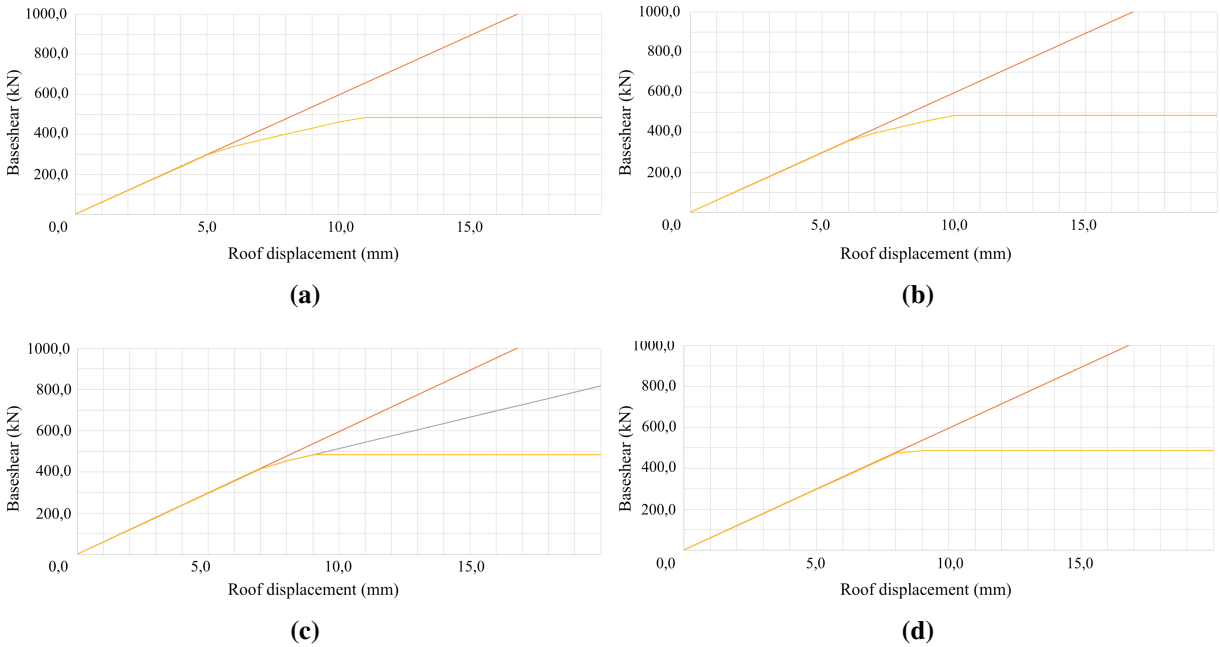

Figure 5.13: Pushover curves where λ is 0,9 and ι is (a) 40-, (b) 30-, (c) 20- and (d) 10 %.

5.4.4.2 30 % reduced capacity of pile 2 and 3, ι

The horizontal springs which belong to support number 1 and 4 are given multilinear properties, which are elastic until the springs are exposed to a lateral load F_y of 147,71 kN. As an effect of reducing the capacity of pile number 2 and 3 with 30 % from the required value of 134,28 kN, the obtained pushover curve is constant until reaching a total base shear of 375,99 kN. This curve is pictured in Figure 5.13 (b).

The earthquake load is estimated to give the roof level a lateral displacement of 7,97 millimetre, which corresponds to a base shear of 425,00 kN in the pushover curve. The calculations are shown in Appendix C. This base shear is below the elastic limit of pile 1 and 4, which are bot getting exposed to a reaction force of 118,50 kN. The utilization ratio of the total system is 0,879 and calculated to be 0,802 for pile 1 and 4. For pile 2 and 3, the utilization is 1,00 since these piles have passed their elastic limit.

5.4.4.3 20 % reduced capacity of pile 2 and 3, ι

The capacity of pile 2 and 3 separately is set to 107,42 kN, which is a 20 % reduction from the design value from section 5.2. The supports number 1 and 4 is given a capacity of 134,28 kN each in order to get a total capacity of 483,4 kN. This gives a pushover curve as illustrated in Figure 5.13 (c).

The calculation of the earthquake load is found in Appendix C. The result is a roof displacement of 7,84 millimetre. This load gives the support system a base shear of 447,00 kN. This gives a reaction force of 116,07 kN for the outer piles, while pile 2 and 3 get exposed to a load of 107 kN each. It is found that pile 1 and 4 have residual capacity, which means that these piles behave elastically. The outer piles are utilized with a ratio of 0,864, while pile 2 and 3 have reached their maximum capacity and given a utilization ratio of 1,0. The utilization ratio of the total system is 0,92.

5.4.4.4 10 % reduced capacity of pile 2 and 3, ι

The horizontal springs in this subsection are given the same capacity, which is 120,85 kN, for obtaining the capacity of 438,4 kN. The spring is kept elastic until the system are given a base displacement of 7,73 millimetre. These properties makes the superstructure behave like illustrated in Figure 5.12 (d).

It is calculated that the earthquake load produces a roof displacement of 7,79 millimetre and base shear of 461,00 kN, which are within the defined elastic range for the system. The calculations are found in Appendix C. The reaction forces from this displacement are 115,25 kN per pile, where every pile is utilized similarly, with a ratio of 0,95.

The development of the utilization ratio of the piles in this subsection is given in Table 5.14. The roof displacement is reduced as a consequence of reducing the difference between the capacity of the piles in the middle and the outer piles. A comparison between Table 5.5, 5.8, 5.11 and 5.14 clarifies that the reduced elasticity gives a reduced roof displacement. The results from this subsection give the lowest roof displacement of all the investigated parameter combinations. From Table 5.15, the ductilization ratio for the system with a capacity 10 $\%$ below the estimation from EC8 is given. Pile 2 and 3 are still obtaining ductilization when the capacity of these piles are given a reduced capacity of 20 $\%$ or more. The ratios in this table indicate plastic behaviour, i.e. above 1,0, but these ratios are lower compared to the equivalent systems with higher capacities.

Table 5.14: Normalized reaction forces and roof displacements from earthquake load when λ is 0,9.

		Normalized force		
ι ($\%$)	d_n (mm)	F1 and F4	F2 and F3	Total
40,0	8,19	0,76	1,0	0,84
30,0	7,97	0,80	1,0	0,879
20,0	7,84	0,86	1,0	0,92
10,0	7,79	0,95	0,95	0,95

Table 5.15: Obtained base displacements and ductility ratios when λ is 0,9.

		Normaliced displacement	
ι ($\%$)	d_0 (mm)	D1 and D4	D2 and D3
40,0	7,83	0,76	1,52
30,0	7,58	0,80	1,26
20,0	7,42	0,86	1,08
10,0	7,37	0,95	0,95

The presented results in this section tell that perfect elastoplastic piles are found to give lower roof displacements to the superstructure when a superstructure is exposed to an earthquake load compared to a system with elastic piles. This might seem to be a contradiction as the pushover curve for the elastic spring supported system, presented in section 5.2, shows that the capacity of this structure is higher than the superstructures with perfect elastoplastic piles. Hence,

a finding which concludes that perfectly elastoplastic spring supported structures, with lower capacity, gives a lower roof displacement requires an explanation. As the determination of the earthquake load for a structure is based on the natural period of an equivalent SDOF system with a lumped mass, the stiffness of this equivalent system is crucial. This because the mass of the systems are equal in all of these cases, as the mode shapes are equal. In section 3.5.2, Figure 3.1 illustrates the idealized perfect elastoplastic force-displacement relationship which the determination of the earthquake load should be based on. Figure 5.14 (a) shows four different pushover curves. The orange curve is the pushover curve for the equivalent SDOF system, and the yellow curve is the bi-linear force-displacement relationship estimated as given in section 3.5.2. The third and fourth curve are identical, where only the blue curve is visible. These two identical curves represent the pushover curve for the equivalent SDOF system for the superstructure supported by springs with perfect elastoplastic properties and the belonging bi-linear curve estimated according to this method. Figure 5.15 (b) shows the total pushover curve for the linear spring supported superstructure. As the stiffness for elastic SDOF systems is equal to the slope of the force-displacement relationship, the system with perfect elastoplastic springs is stiffer than the system supported by linear spring. Because the method for determination of the earthquake load defines the linear spring supported system to be softer than the perfect elastoplastic system, it is reasonable to consider the observed results in this section to be correct.

Superstructures exposed to earthquake load and supported by perfect elastoplastic piles obtain the stress distribution, as shown in Figure 5.15. Figure (a) represents a system with 30 $\%$ capacity margin and (b) a system with a capacity of 10 $\%$ below the desired value. In other words, the figures illustrate the spectrum of the investigated superstructure supported by springs with bi-linear properties and a 40 $\%$ reduced capacity of pile 2 and 3. The stress distributions are from the reinforcement layer of the SAP2000 models. The magnitude of the tensile stresses is at a level where the structure is kept intact.

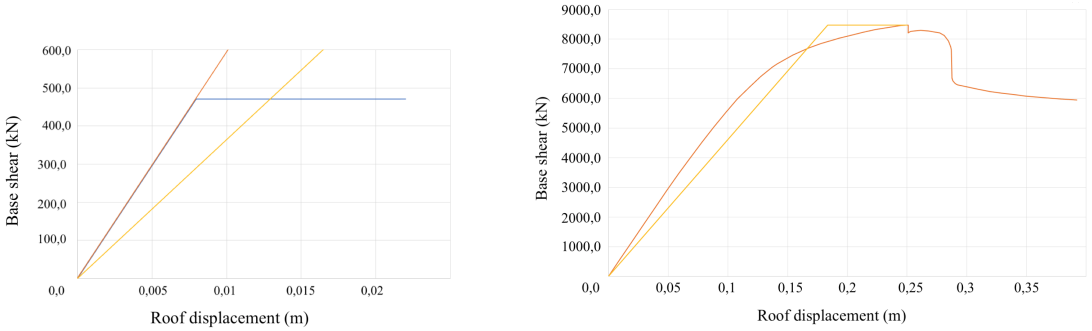

(a) **(b)**

Figure 5.14: Comparison between the applied curves for the determination of the earthquake load from the systems in section 5.4.4.4 and 5.2 .

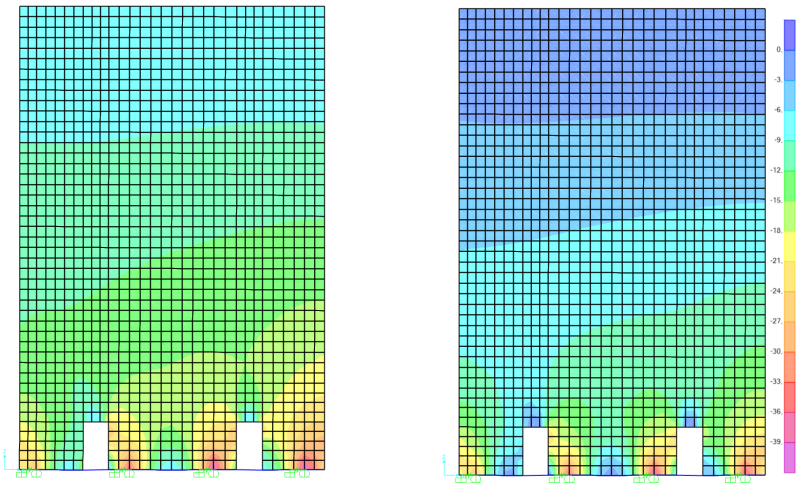

(a) **(b)**

Figure 5.15: Stress distribution for a structure supported by bi-linear springs, where pile 2 and 3 are given 40 % reduced capacity; The systems has a (a) 30 % capacity margin; (b) capacity 10 % below the desired value.

Chapter 6

Discussion & Conclusion

6.1 Discussion

Reflection of the results is necessary in order to find out whether piles designed with properties where ductile behaviour gives acceptable results. Firstly, the reliability of the results is discussed. Secondly, the results from each of the global utilization ratios λ are evaluated. Finally, general findings have been found by comparing the outcome of the different λ values. This leads to the conclusions in section 6.2.

6.1.1 Reliability of the simulated models

In order to investigate a system which allows ductile behaviour of the piles, it is necessary to clarify whether the system is behaving realistically. This is because physical test results to compare and verify the results from the analyses is not available. It is observed that the superstructure is given an increased natural period, from 0,35 to 0,79 seconds, as a consequence of implementing the linear springs to the horizontal support. This development is supported by the research work conducted both by Sharma et al. (2018) and Bi et al. (2011). The capacity of the system, which is horizontally supported by linear springs, also get an increased capacity. This happens because an evenly distributed load is favourable compared to the inverted triangular load distribution from the pinned supported superstructure. The determined earthquake load is increased as a consequence of changing the support system from pinned to roller supports combined with a horizontal linear spring. The change of the supports reduces the stiffness of the idealized equivalent SDOF system. The implementation of plastic behaviour is done by inserting springs with bi-linear behaviour, which is equal to a perfect elastoplastic property. The combination of applying two elastic piles and two perfect elastoplastic piles gave

a pushover curve identical to the elastic spring supported superstructure up to the point where all the springs where still kept within the elastic range. After reaching this point, the pushover curve of the system combining elastic and perfect elastoplastic properties had a reduced slope. This reduction can be explained by that the stiffness of the support has been halved since the stiffness of the middle piles is zero from this point of the capacity curve. This system represents the system with the highest roof displacement as a consequence of the determined earthquake load. These presented results indicate that the system is properly modelled.

6.1.2 Global utilization ratio λ of 1,3

This section is related to the findings from Table 5.5 and 5.6. These tables show that pile 1 and 4 behaves elastically in all the examined cases. The elastic range of the perfect elastoplastic spring property is determined by the design parameter λ, which has a value of 1,3. This equals a total capacity of 698,26 kN, given in Table 5.3. The consequence of the λ value in this section is that the perfect elastoplastic piles 2 and 3 get permanently deformed since these are designed with reduced capacity, ι. When the load and displacement exceed the point of yielding, which is controlled by the value of ι, the piles 2 and 3 can not resist any further loads. At this point, the system relies on the capacity of pile 1 and 4. As these piles are capable of handling far more load than the piles which has yielded, these continue to carry the horizontal load from the earthquake. Consequently, the yielded piles, with number 2 and 3, follows the movement of the basement without any resistance. This statement is supported by the normalized displacements collected in Table 5.6. In this table, it is shown that the values of ι and the ductility ratios develop in the same direction. Because the ductility ratio of pile 2 and 3 is 1,65, when ι is 40 $\%$, these piles probably have reduced material properties. However, since pile 1 and 4 still have a utilization ratio of 0,49, they have linear properties. This makes the total utilization ratio from Table 5.5 become 0,61, where the system still has the capacity to remain in a stable state. The disadvantage of a support system like this is that it gets soft properties as a consequence of being horizontally supported by a halved amount of piles. For a superstructure with piles given a reduction ι of 10 $\%$, the outcome of the seismic event is improved. The roof displacement is reduced from 8,80 to 8,14 millimetre, which reduces the damage of the superstructure. On the other hand, the total utilization ratio is increased to 0,69. This gives a total base shear of 483,4 kN. This combination also gives a ductility ratio of pile 2 and 3 of 0,99. Therefore, these piles are at the threshold related to elastic behaviour. Nevertheless, the earthquake has not caused the system to start yielding. This makes the total support system to return to its original position after the seismic event has happened.

6.1.3 Global utilization ratio λ of 1,2

By choosing to design a system with an λ value of 1,2 the total capacity gets 644,55 kN, from Table 5.3. Combined with the given values of reduced capacities, ι, this yields the Tables 5.8 and 5.9. These tables brief that when ι is 40 $\%$ the system obtain a utilization ratio of 0,53 for pile 1 and 4 as a consequence of exposing the system to an earthquake. This is a sufficient result, where the piles behave elastically. These piles have been designed with a capacity of 241,71 kN to achieve the desired λ value in this section. Elastic behaviour is not found for piles 2 and 3. These piles have reached their maximum elastic capacity, which is pointed out from Table 5.9. The result of this table is that the ductility ratio is 1,61. It is, however, reasonable to declare this system to be stable since the total utilization ratio is 0,65. Nevertheless, this system gets only supported by pile 1 and 4, as the other two piles have yielded and have become inelastic. A similar system where ι is reduced to 10 $\%$, gives a utilization ratio of 0,98 for pile 2 and 3. This means that the pile respond elastically to the earthquake, at the upper part of the elastic range. These piles are the ones with the lowest capacity. Since it is sensible to claim that these piles have sufficient capacity, this means that nether pile 1 and 4 nor the system in total will be given permanent displacement. This result is probably related to increased stiffness of the system, where the base displacement is decreased from 8,28 to 7,61 millimetre. Table 5.9 shows that the decreased base displacement corresponds to a decreased ductility ratio of pile 2 and 3. This reduction is sensible to connect with increased stiffness, as the total capacity of the system has been held constant while the base displacement is decreased.

6.1.4 Global utilization ratio λ of 1,1

The outcome of giving the pile supports a λ value of 1,1 is given in Table 5.11 and 5.12 and the total horizontal capacity of 590,84 kN is listed in Table 5.3. This base shear capacity is lower than the other investigated systems mentioned until now. A natural result of this reduced capacity is that the ductility ratios for pile 2 and 3 are decreased. The outcome is that the pile number 2 and 3 obtains less permanent displacements compared to the examined cases where λ has a value of 1,3 and 1,2. These values are given in Table 5.12. When the system is designed with an λ value of 1,1, and a ι of 40 $\%$, the total utilization ratio gets 0,70. This result occurs despite the fact that pile 2 and 3 have been given permanent displacements. Since pile 2 and 3 do not contribute to resist any further load and behave plastically, there is no possibility for the system to get back to the original position. Such a withdrawal requires elastic behaviour of all of the piles. As the total utilization ratio is below 1,0 and pile 1 and 4 has a utilization ratio of

0,59, it is reasonable to claim that the system still remains stable. When the global utilization ratio λ is 1,1 and the ι is 10 $\%$, the system remain completely elastic. This is among others registered on the basis that every ductility ratio is below 1,0.

6.1.5 Global utilization ratio λ of 0,9

This section is investigating the results from analyzes, where the total support system has a global utilization ratio of λ of 0,9. Table 5.3 tells that the total capacity is 483,41 kN. This value has a capacity 10 $\%$ bellow what is calculated to be necessary for a system where the piles behave elastically. Designing the system with a λ of 0,9 combined with the highest reduction of pile 2 and 3, i.e. ι equal 40 $\%$, gives a ductility ratio of 1,52 for pile 2 and 3. Consequently, pile 1 and 4 are contributing in order to compensate for the piles which have yielded. This is possible because the utilization ratio of pile 1 and 4 are below 1,0, which means that these piles have not reached their maximum capacity. Pile 2 and 3 have reached their maximum capacity and behaves perfectly plastically as a result of the ductility ratio of 1,52. However, since the total utilization ratio is equal 0,84, the system could still endure more horizontal loading. By investigating the case where the reduction ι equals 10 $\%$, the pile supports as a total system gets utilized with a ratio of 0,95. This means that the system remains stable after the seismic event has happened. The properties of the piles are all being elastic, as shown in Table 5.15. The same result could be found by examining the pushover curve from Figure 5.13 (d). This pushover curve shows that the total support system follows a constant slope until reaching the point of yielding.

6.1.6 Comparison between the different λ values

In this section, the behaviour of the superstructure and the pile supports is compared between the different utilization ratios, λ. This could lead to general findings. The order of magnitude given to λ defines the size of the elastic range. This finding is based on the values given in Table 5.3. All of the systems are found to be stable, as the total utilization ratio does not exceed 1,0 in any of the cases. One general tendency is that the roof displacement decreases as a consequence of changing λ to a lower order of magnitude. This requires that the ι is held constant, as an increase of this parameter gives a larger roof displacement. The effect of reducing the value of ι is that the supports 2 and 3 obtains a higher degree of capacity. This gives the system a higher stiffness. On the other hand, an increased value of λ only makes the total utilization ratio to decrease. This is important for the system which does not obtain elastic properties since they are left with a permanently reduced displacement of the system. If the

system is rigid, like the investigated system in this thesis is found to be, the roof displacement does not change much. Therefore, giving the system a λ value of 1,3 together with a ι of 40 $\%$ does still not make the roof displacement larger than what is found for the system supported by elastic piles. This would give the lowest utilization ratio of all the investigated systems, which is useful because the system has been left with inelastic behaviour and a permanent displacement. Consequently, if the system should be designed to be left with inelastic properties, this system would be the one to prefer. However, this strategy requires larger pile dimensions for the piles, which remains elastic compared to what is necessary if the system is designed with elastic piles.

If the designer wants to obtain a pile system with elastic properties after the seismic event has occurred, related to the requirement of elastic behaviour from EC8, the system could be designed with all the investigated λ values. However, the system needs to be given natural properties which keeps the piles to remain elastic. In the conducted parameter study, this happens when the system has a reduced capacity of pile 2 and 3, ι, of 10 $\%$. If the designer wants to save money through designing a structure with small piles, the system should be designed with λ values of 0,9. The reason for this claim is that the needed capacity of the piles is at the lowest if choosing this capacity. The other λ options give the system lower total utilization ratios, but the utilization ratio of pile 2 and 3 increases along with the increased value of λ. Since the support system remains elastic in general when ι is 10 $\%$, the supports will return to its original shape. Therefore, the designer could choose any of the λ values and still be sure that the system has sufficient behaviour if an earthquake occurs. With a climate and economic perspective though, the designer should seek to reduce the material usage. This perspective would make the designer choose the system which utilizes the system the most. As this happens when λ is 0,9, this system should be chosen. This alternative is also beneficial regarding the roof displacement, which is at the lowest of all the investigated systems. A λ value of 0,9 gives the system with the lowest designed elastic range, and the preferred alternative presented is the system with the highest stiffness. This indicates that designing the support system with perfect elastoplastic piles, in general, is better than a system designed with piles that remain elastic throughout the pushover curve. This requires an elastic range 10 $\%$ below the requirement of the elastic designed system together with high total stiffness. The needed stiffness is achieved by giving the system an equal capacity. The conclusion is stated based on the observation that a bi-linear supported system with high total stiffness is found to remain elastic.

6.2 Conclusion

The research objective in this thesis was to investigate whether designing for inelastic behaviour of piles exposed to an earthquake gives acceptable results regarding the structural behaviour. This has been investigated through comparing the structural behaviour of a superstructure supported by elastic piles with an identical superstructure supported by piles designed with perfect elastoplastic properties. The requirement from EC8, that piles should be designed to remain elastic, is related to the input properties for the pushover curve and not the outcome of the earthquake event. The structural behaviour that is compared is the result of the method for determination of the earthquake load, presented in EC8 part 1. This method applies the results from the static pushover curve where the load is based on the first mode shape from the modal analysis. The superstructure, supported by perfect elastoplastic piles, has been investigated through a parameter study. This was done by changing the total elastic range of the support system. The elastic range was changed based on the demanded capacity of the superstructure supported by elastic piles. Each chosen capacity was divided into cases where two of the piles were given a reduced capacity.

The conducted parameter study has found that piles with perfect elastoplastic properties can be advantageous under certain conditions. One general benefit is that the roof displacement gets reduced by using perfect elastoplastic piles instead of elastic piles. The observations that have been made also indicate that perfect elastoplastic piles remain elastic if the supports collectively are given sufficient stiffness. Combined with the lowest global ductility ratio in the parameter study, the support with sufficient stiffness for the total system gives elastic piles with lower reaction forces than piles designed to remain elastic. It has also been found that none of the investigated systems in the parameter study become unstable, even though some of the piles got permanently displaced. These main findings indicate that piles with ductile behaviour included in the description of design properties gives improvements to the system compared to piles designed to remain elastic. These improvements are decreased roof displacement, reduced required capacity and piles which remain elastic after the seismic event has occurred. The conducted investigation concludes that designing for inelastic behaviour of piles exposed to an earthquake seems to improve the response of the structure, given certain conditions. Therefor, this thesis concludes that it is reasonable to claim that designing for inelastic behaviour gives acceptable results regarding the requirements from EC8.

6.2.1 Further work

This thesis has investigated the structural behaviour of a shear wall designed with inelastic behaving piles. As the topic in this thesis is extensive and complex, further research work is required in order to make sure that the results have general validity. The findings are based on the results from one parameter study and related to one specific case study. This makes it likely that nuances have not been uncovered. By doing more simulations of superstructures with other properties, e.g. less rigidity or change of material, would help to increase the knowledge related to inelastic designed piles. The analyzes were conducted in 2D, where the impact from the entire building is not included. Hence, the out of plane deflection of the shear wall has not been investigated, nor the stabilizing effect from the other structural elements. This is proposed research work which would expand the knowledge related to inelastic pile supports further.

Bibliography

N. Standard, "Ns-en 1998-1: 2004+ a1: 2013+ na2014," *Eurocode 8: Design of structures for earthquake resistance. Part 1: General rules, seismic actions and rules for buildings*, 2004.

B. B. Broms, "Lateral resistance of piles in cohesive soils," *Journal of the Soil Mechanics and Foundations Division*, vol. 90, no. 2, pp. 27–63, 1964a.

A. Rønnquist, T. Karlson, and S. Remseth, "Earthquake design practice of traditional norwegian buildings according to eurocode 8," 2012.

B. EN *et al.*, "Eurocode 8: Design of structures for earthquake resistance-part 5: Foundations, retaining structures and geotechnical aspects." 2004.

B. B. Broms, "Lateral resistance of piles in cohesionless soils," *Journal of the Soil Mechanics and Foundations Division*, vol. 90, no. 3, pp. 123–156, 1964b.

F. Kulhawy and Y. Chen, "A thirty year perspective of broms' lateral loading models, as applied to drilled shafts," in *Proceedings, Bengt B. Broms Symposium in Geotechnical Engineering*, 1995, pp. 13–15.

M. Pender, "Aseismic pile foundation design analysis," *Bulletin of the New Zealand Society for Earthquake Engineering*, vol. 26, no. 1, pp. 49–160, 1993.

M. Budhu and T. G. Davies, "Analysis of laterally loaded piles in soft clays," *Journal of geotechnical engineering*, vol. 114, no. 1, pp. 21–39, 1988.

L. C. Reese, W. R. Cox, and F. D. Koop, "Analysis of laterally loaded piles in sand," *Offshore technology in civil engineering hall of fame papers from the early years*, pp. 95–105, 1974.

G. Gazetas and N. Makris, "Dynamic pile-soil-pile interaction. part i: analysis of axial vibration," *Earthquake Engineering & Structural Dynamics*, vol. 20, no. 2, pp. 115–132, 1991.

S. Jarernprasert, E. Bazan-Zurita, and J. Bielak, "Seismic soil-structure interaction response of inelastic structures," *Soil Dynamics and Earthquake Engineering*, vol. 47, pp. 132–143, 2013.

P. Raychowdhury, "Seismic response of low-rise steel moment-resisting frame (smrf) buildings incorporating nonlinear soil–structure interaction (ssi)," *Engineering Structures*, vol. 33, no. 3, pp. 958–967, 2011.

N. Sharma, K. Dasgupta, and A. Dey, "Natural period of rc buildings considering seismic soil structure interaction effects," 2018.

K. Bi, H. Hao, and N. Chouw, "Influence of ground motion spatial variation, site condition and ssi on the required separation distances of bridge structures to avoid seismic pounding," *Earthquake Engineering & Structural Dynamics*, vol. 40, no. 9, pp. 1027–1043, 2011.

M. El Naggar and M. Novak, "Nonlinear analysis for dynamic lateral pile response," *Soil Dynamics and Earthquake Engineering*, vol. 15, no. 4, pp. 233–244, 1996.

A. K. Chopra and R. K. Goel, "Capacity-demand-diagram methods for estimating seismic deformation of inelastic structures: Sdf systems," *Report No. PEER1999/02*, 1999.

M. J. Skokan and G. C. Hart, "Reliability of nonlinear static methods for the seismic performance prediction of steel frame buildings," in *Proceedings of the 12th World Conference on Earthquake Engineering*, 2000.

A. Gupta and H. Krawinkler, "Seismic demands for the performance evaluation of steel moment resisting frame structures," Ph.D. dissertation, Stanford University, 1998.

H. Krawinkler and G. Seneviratna, "Pros and cons of a pushover analysis of seismic performance evaluation," *Engineering structures*, vol. 20, no. 4-6, pp. 452–464, 1998.

A. Mwafy and A. S. Elnashai, "Static pushover versus dynamic collapse analysis of rc buildings," *Engineering structures*, vol. 23, no. 5, pp. 407–424, 2001.

S. Kunnath and E. Erduran, "Pushover procedures for seismic assessment of buildings: Issues, limitations and future needs," 2008.

T. Davies and M. Budhu, "Non-linear analysis of laterally loaded piles in heavily overconsolidated clays," *Geotechnique*, vol. 36, no. 4, pp. 527–538, 1986.

M. Budhu and T. G. Davies, "Nonlinear analysis of laterality loaded piles in cohesionless soils," *Canadian Geotechnical Journal*, vol. 24, no. 2, pp. 289–296, 1987.

S. K. Kunnath, A. M. Reinhorn, and Y. J. Park, "Analytical modeling of inelastic seismic response of r/c structures," *Journal of Structural Engineering*, vol. 116, no. 4, pp. 996–1017, 1990.

M. Ciampoli and P. E. Pinto, "Effects of soil-structure interaction on inelastic seismic response of bridge piers," *Journal of structural engineering*, vol. 121, no. 5, pp. 806–814, 1995.

D. Badoni and N. Makris, *Analysis of the nonlinear response of structures supported on pile foundations*. Earthquake Engineering Research Center, University of California, 1997.

R. Bouc, "Modèle mathématique d'hystérésis," *Acustica*, vol. 21, pp. 16–25, 1971.

A. Chopra, *Dynamics of Structures: Theory and Applications to Earthquake Engineering*, ser. Always learning. Pearson, 2017. [Online]. Available: https://books.google.no/books?id=R8_XjwEACAAJ

J. Jia, *Soil dynamics and foundation modeling*. Springer, 2018.

J. P. Stewart, G. L. Fenves, and R. B. Seed, "Seismic soil-structure interaction in buildings. i: Analytical methods," *Journal of Geotechnical and Geoenvironmental Engineering*, vol. 125, no. 1, pp. 26–37, 1999.

S. Helwany, *Applied soil mechanics with ABAQUS applications*. John Wiley & Sons, 2007.

B. McClelland *et al.*, "Soil modulus for laterally loaded piles," *Journal of the Soil Mechanics and Foundations division*, vol. 82, no. 4, pp. 1–22, 1956.

L. C. Reese, W. R. Cox, F. D. Koop *et al.*, "Field testing and analysis of laterally loaded piles on stiff clay," in *Offshore Technology Conference*. Offshore Technology Conference, 1975.

B. B. Broms, "Lateral resistance of piles in cohesive soils," *Journal of the Soil Mechanics and Foundations Division*, vol. 90, no. 2, pp. 27–63, 1964.

G. Vining, "Technical advice: Scientific method and approaches for collecting data," *Quality Engineering*, vol. 25, no. 2, pp. 194–201, 2013.

T. Grenness, *Innføring i vitenskapsteori og metode*. Tano Aschehoug, 1997.

L. Christoffersen and A. Johannessen, *Forskningsmetode for lærerutdanningene*. Abstrakt, 2012.

E. Winsberg, "Simulated experiments: Methodology for a virtual world," *Philosophy of science*, vol. 70, no. 1, pp. 105–125, 2003.

W. L. Oberkampf and C. J. Roy, *Verification and validation in scientific computing*. Cambridge University Press, 2010.

S. CSI, "Analysis reference manual," *CSI: Berkeley (CA, USA): Computers and Structures Inc*, 2019.

Z.-F. Fu and J. He, *Modal analysis*. Elsevier, 2001.

S. Norway, "Ns-en 1991-1-1: 2002+ na: 2008," in *Eurocode*, vol. 1, 2008, pp. 1–2.

——, "Eurocode 1: Laster på konstruksjoner; del 1-3: Almenne laster; snølaster," *NS-EN 1991-1-3: 2003+ NA*, 2008.

Appendix A

- Part 1

	Load distribution – Area division of the shear wall (kN/m^2)								
	Area	Floor6	Floor2-5	Area	Floor1	Area	Basement - upper	Area	Basement - lower
Dead load	2,05	11,280488	11,2804878	2,04	11,3357843	1,26	18,3531746	1,56	14,82371795
Added dead load		0,902439	3,15853659		3,17401961		5,138888889		4,150641026
Service load		5,7756098	3,6097561		3,62745098		5,873015873		4,743589744
Dead load	5,73	11,261998	11,2619983	5,68	11,3611356	3,51	18,38497151	4,38	14,7331621
Added dead load		0,9009599	3,15335951		3,18111796		5,147792023		4,125285388
Service load		5,7661431	3,60383944		3,63556338		5,883190883		4,714611872
Dead load	3,11	11,254019	11,2540193	3,08	11,3636364	1,9	18,42105263	-	-
Added dead load		0,9003215	3,1511254		3,18181818		5,157894737		
Service load		5,7620579	3,60128617		3,63636364		5,894736842		
Dead load	2,54	11,257382	11,2573819	2,52	11,3467262	1,56	18,32932692	1,94	14,73904639
Added dead load		0,9005906	3,15206693		3,17708333		5,132211538		4,12693299
Service load		5,7637795	3,6023622		3,63095238		5,865384615		4,716494845
Dead load	10,32	11,264535	11,2645349	10,23	11,3636364	6,32	18,39398734	7,89	14,7338403
Added dead load		0,9011628	3,15406977		3,18181818		5,150316456		4,125475285
Service load		5,7674419	3,60465116		3,63636364		5,886075949		4,714828897
Dead load	2,86	11,265297	11,2652972	2,84	11,3446303	1,75	18,41071429	2,19	14,71175799
Added dead load		0,9012238	3,15428322		3,17649648		5,155		4,119292237
Service load		5,7678322	3,6048951		3,63028169		5,891428571		4,707762557
Dead load	3,11	11,254019	11,2540193	3,08	11,3636364	1,9	18,42105263	-	-
Added dead load		0,9003215	3,1511254		3,18181818		5,157894737		
Service load		5,7620579	3,60128617		3,63636364		5,894736842		
Dead load	5,16	11,258479	11,2584787	5,111	11,3664156	3,16	18,3840981	3,94	14,7446066
Added dead load		0,9006783	3,15237403		3,18259636		5,147547468		4,128489848
Service load		5,7643411	3,60271318		3,63725298		5,882911392		4,718274112
Dead load	2,41	11,345954	11,3459544	2,39	11,4408996	1,48	18,47550676	1,84	14,8607337
Added dead load		0,9076763	3,17686722		3,20345188		5,173141892		4,161005435
Service load		5,8091286	3,63070539		3,66108787		5,912162162		4,755434783

- Part 2

Applied mass for the determination of the earthquake load

Roof			Point load	
Reinforced concrete	25,0	kN/m3	93,225	kN
Dead load - concrete floor	6,25	kN/m2	420	kN
Added dead load	0,5	kN/m2	33,6	kN
Snow load	3,2	kN/m2	215,04	kN
			761,865	kN
		Total mass	77,66207951	t

2.-6. Floor				
Reinforced concrete	25,0	kN/m3	186,45	kN
Dead load - concrete floor	6,25	kN/m2	420	kN
Added dead load	1,75	kN/m2	117,6	kN
Service load	2,0	kN/m2	134,4	kN
			858,45	kN
		Total mass	87,50764526	t

1. Floor			Point load	
Reinforced concrete	25,0	kN/m3	232,55	kN
Dead load - concrete floor	6,25	kN/m2	420	kN
Added dead load	1,75	kN/m2	117,6	kN
Service load	2,0	kN/m2	134,4	kN
			904,55	kN
		Total mass	92,2069317	t

Basement				
Reinforced concrete	25,0	kN/m3	140,55	kN
Dead load - concrete floor	7,65	kN/m2	514,08	kN
Added dead load	4,0	kN/m2	268,8	kN
Service load	2,0	kN/m2	134,4	kN
			1057,83	kN
		Total mass	107,8318043	t

Volumes applied for converting the volume load to point load are:

Roof: 3,729 m^3

2.-6. Floor: 7,458 m^3

1. Floor: 9,302 m^3

Basement: 5,622 m^3

Area applied for converting the area load to point load: 67,2 m^2

Appendix B

Applied nonlinear properties for the reinforcement

Strain (mm)	Stress (MPa)
-0,072	-449,5
-0,06	-689,5
-0,0294	-632
-0,0111	-574,6
-5,0E-03	-517,1
-2,59E-03	-517,1
0	0
2,59E-03	517,1
5,00E-03	517,1
0,0111	574,6
0,0294	632
0,06	689,5
0,072	449,5

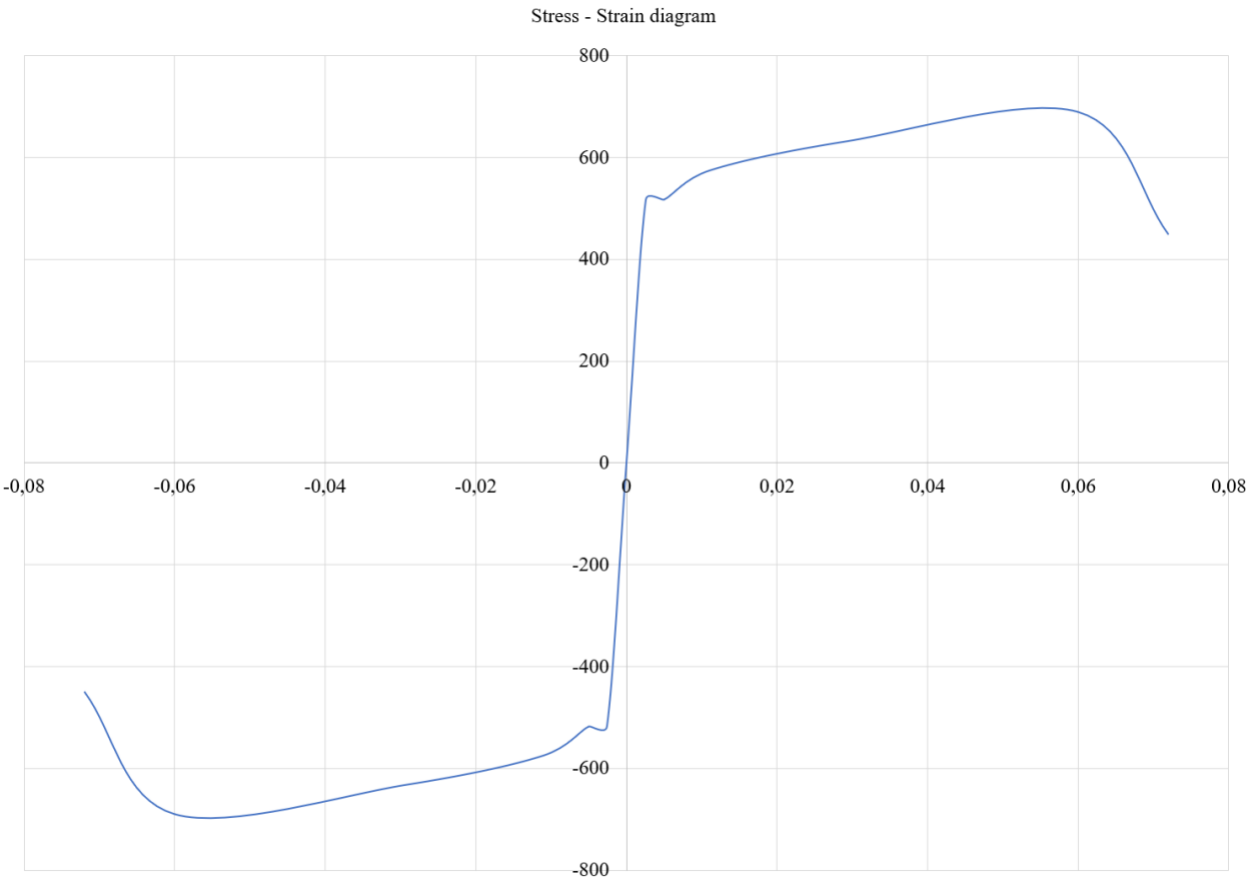

Applied nonlinear properties for the confined concrete

Strain (mm)	Stress (MPa)
-8,89E-03	-28,0389
-6,67E-03	-28,0389
-2,89E-03	-37,3848
-1,78E-03	-37,3848
-5,8E-04	-21,4503
0,00E+00	0
5,76E-10	2,14E-05
4,44E-03	2,14E-05

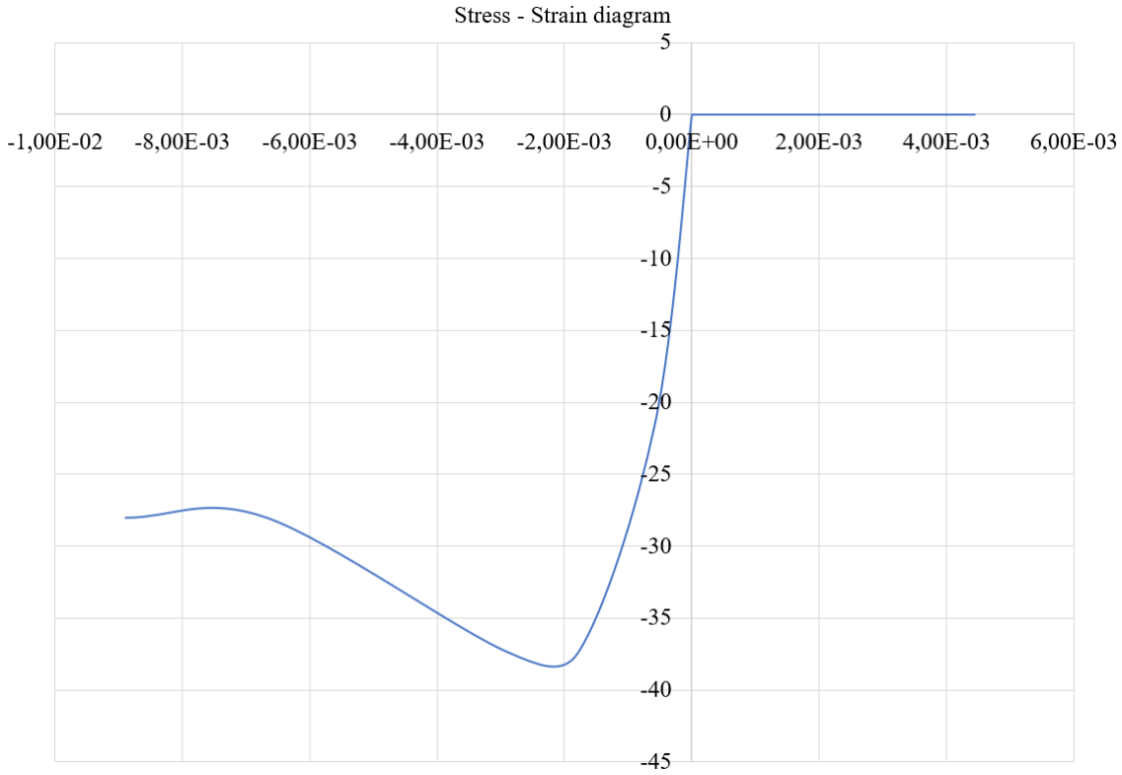

Appendix C

Calculation of target displacement, from EC8 – part 1, Appendix B.

Multilinear springs

30% capacity margin

- 40% reduced capacity of Pile 2 and 3

E_m (kNm)	d^*_y (m)	T* (s)	d^*_{et} (m)	d_n (m)
6,8462	0,0146	0,7695	0,008576	0,008801

- 30% reduced capacity of Pile 2 and 3

E_m (kNm)	d^*_y (m)	T* (s)	d^*_{et} (m)	d_n (m)
6,6150	0,0137	0,7442	0,008294	0,008512

- 20% reduced capacity of Pile 2 and 3

E_m (kNm)	d^*_y (m)	T* (s)	d^*_{et} (m)	d_n (m)
6,2656	0,0131	0,7277	0,008111	0,008324

- 10% reduced capacity of Pile 2 and 3

E_m (kNm)	d^*_y (m)	T* (s)	d^*_{et} (m)	d_n (m)
5,8727	0,0125	0,7114	0,007929	0,008137

20% capacity margin

- 40% reduced capacity of Pile 2 and 3

E_m (kNm)	d^*_y (m)	T* (s)	d^*_{et} (m)	d_n (m)
5,7446	0,01312	0,7579	0,008447	0,008669

- 30% reduced capacity of Pile 2 and 3

E_m (kNm)	d^*_y (m)	T* (s)	d^*_{et} (m)	d_n (m)
5,5431	0,0122	0,7322	0,00816	0,008374

- 20% reduced capacity of Pile 2 and 3

E_m (kNm)	d^*_y (m)	T* (s)	d^*_{et} (m)	d_n (m)
5,0936	0,0117	0,7162	0,007982	0,008192

- 10% reduced capacity of Pile 2 and 3

E_m (kNm)	d^*_y (m)	T* (s)	d^*_{et} (m)	d_n (m)
4,7362	0,0112	0,7014	0,007817	0,008022

10% capacity margin

- 40% reduced capacity of Pile 2 and 3

E_m (kNm)	d^*_y (m)	T* (s)	d^*_{et} (m)	d_n (m)
4,6978	0,0116	0,7451	0,008305	0,008522

- 30% reduced capacity of Pile 2 and 3

E_m (kNm)	d^*_y (m)	T* (s)	d^*_{et} (m)	d_n (m)
4,3957	0,0109	0,7228	0,008056	0,008267

- 20% reduced capacity of Pile 2 and 3

E_m (kNm)	d^*_y (m)	T* (s)	d^*_{et} (m)	d_n (m)
4,080876	0,010403	0,705001	0,007857	0,008064

- 10% reduced capacity of Pile 2 and 3

E_m (kNm)	d^*_y (m)	T* (s)	d^*_{et} (m)	d_n (m)
3,7224	0,01002	0,6920	0,0077	0,0079

10% below required capacity margin

- 40% reduced capacity of Pile 2 and 3

E_m (kNm)	d^*_y (m)	T* (s)	d^*_{et} (m)	d_n (m)
2,8778	0,00878	0,7162	0,00798	0,008191

- 30% reduced capacity of Pile 2 and 3

E_m (kNm)	d^*_y (m)	T* (s)	d^*_{et} (m)	d_n (m)
2,6046	0,0083	0,6969	0,0078	0,007971

- 20% reduced capacity of Pile 2 and 3

E_m (kNm)	d^*_y (m)	T* (s)	d^*_{et} (m)	d_n (m)
2,2361	0,00802	0,6850	0,007635	0,007835

- 10% reduced capacity of Pile 2 and 3

E_m (kNm)	d^*_y (m)	T* (s)	d^*_{et} (m)	d_n (m)
1,9007	0,00795	0,6812	0,007592	0,007791